Redox Biology 8 (2016) 226–242

Contents lists available at ScienceDirect

Redox Biology

journal homepage: www.elsevier.com/locate/redox

Research Paper

In vivo evaluation of different alterations of redox status by studying pharmacokinetics of nitroxides using magnetic resonance techniques

Goran Bačić [a,*], Aleksandra Pavićević [a], Fabienne Peyrot [b,c]

[a] EPR Laboratory, Faculty of Physical Chemistry, University of Belgrade, 11000 Belgrade, Serbia
[b] LCBPT, UMR 8601 CNRS - Université Paris Descartes, Sorbonne Paris Cité, 75006 Paris, France
[c] ESPE of Paris, Paris Sorbonne Université, 75016 Paris, France

ARTICLE INFO

Article history:
Received 25 September 2015
Accepted 25 October 2015
Available online 14 November 2015

Keywords:
Reactive oxygen species (ROS)
Redox state
Magnetic resonance imaging (MRI)
Electron paramagnetic resonance (EPR)
Nitroxides
Pharmacokinetics

ABSTRACT

Free radicals, particularly reactive oxygen species (ROS), are involved in various pathologies, injuries related to radiation, ischemia-reperfusion or ageing. Unfortunately, it is virtually impossible to directly detect free radicals *in vivo*, but the redox status of the whole organism or particular organ can be studied *in vivo* by using magnetic resonance techniques (EPR and MRI) and paramagnetic stable free radicals – nitroxides. Here we review results obtained *in vivo* following the pharmacokinetics of nitroxides on experimental animals (and a few in humans) under various conditions. The focus was on conditions where the redox status has been altered by induced diseases or harmful agents, clearly demonstrating that various EPR/MRI/nitroxide combinations can reliably detect metabolically induced changes in the redox status of organs. These findings can improve our understanding of oxidative stress and provide a basis for studying the effectiveness of interventions aimed to modulate oxidative stress. Also, we anticipate that the *in vivo* EPR/MRI approach in studying the redox status can play a vital role in the clinical management of various pathologies in the years to come providing the development of adequate equipment and probes.

1. Introduction

Reactive oxygen species (ROS) are generated constantly in living cells. Their overall effect on cells and tissues is determined by the rate of their production and the concentration of low-molecular-weight antioxidants and activity of enzymatic antioxidants which is often described as the redox state or bioreductive capacity of the system (buffer capacity) [1]. Numerous factors can influence the redox state, either by decreasing antioxidant capacity (redox buffer capacity) or increasing the rate of ROS production, both leading to the enhanced oxidative damage of cells and tissues. Oxidative stress has been implicated in a number of pathological conditions such as ischemia, diabetes, neurological disorders, but it can also be a consequence of external factors such as irradiation, intoxication, use of prescribed and other drugs, etc. [2].

It is no surprise, therefore, that numerous studies have been performed while studying ROS in trying to understand the underlying mechanisms with the ultimate goal of preventing or minimizing their deleterious action. Studies of indirect ROS detection range from assessment of the oxidative products (DNA/RNA damage, lipid peroxidation) through measurements of the antioxidant defense system (SOD, glutathione, etc.) to behavioral studies. An ideal technique should be able to directly and non-invasively measure ROS *in vivo*. Spectroscopic techniques that can measure free radicals using probes or directly have been reviewed [3]. Techniques such as fluorescence and luminescence are widely used for studying cells and tissues *in vitro*, but are hardly applicable for *in vivo* studies due to the low penetration depth of used light. Electron paramagnetic resonance (EPR) has advantages since it can, in principle, detect ROS directly and the used electromagnetic waves have sufficient penetration depth for *in vivo* studies, but the situation is not that ideal in real circumstances.

Zavoyski [4] discovered EPR (also called electron spin resonance, ESR) in 1946, almost at the same time when nuclear magnetic resonance (NMR) was discovered. Both techniques were intended as a tool for investigation in solid state physics, but they soon were employed in studying biological/biochemical systems. The early studies were influenced by the low sensitivity of available EPR spectrometers and difficulties in overcoming the problem of non-resonant absorption of microwaves by watery samples. Nevertheless, efforts to study cells and tissues by EPR continued, mostly motivated by the speculations that enzymatic reactions involve the creation of free radicals and that free radicals might be involved in the development of cancer, so that by 1970s EPR became a well-established and respectable technique in the field of biological/biochemical research.

* Corresponding author.

http://dx.doi.org/10.1016/j.redox.2015.10.007

However, *in vivo* experiments were still beyond reach. The development of the loop-gap resonator in 1982 [5] turned out to be a major breakthrough for *in vivo* EPR. This was soon accompanied by the development of a resonant cavity resonator suitable for whole body experiments on mice [6]. Application of EPR to *in vivo* biological systems essentially started as development of EPR imaging (EPRI) [7,8]. In parallel, extensive work on models and *in vitro* samples has been conducted in establishing basic principles of imaging techniques, contrast enhancement and image reconstruction [9–13]. All this work has been performed by adding external paramagnetic agents, nitroxides (see Section 3), since biological systems do not produce sufficient amounts of radicals to be detected *in vivo*. Next, the first *in vivo* pharmacokinetic experiment has been performed using EPR spectroscopy (EPRS), where injected nitroxides were used to probe redox processes [14]. All these experiments stimulated development of different EPR machines suitable for *in vivo* experiments, and which is equally important, synthesis of new nitroxides that can fulfil specific needs for *in vivo* experiments [15–22]. These articles have been mostly aimed at demonstrating that it is feasible to study the pharmacokinetics of nitroxides, but soon these were followed by studies where the influence of different pathologies on the redox status were investigated (see Section 5). Since the early 90s the field of *in vivo* EPR has grown tremendously in the next two decades to the extent that a complete volume of Biological Magnetic Resonance was needed to cover all the advances and techniques [23]. Much of this work has been stimulated by the discovery that the rate of reduction of nitroxides in cells and tissues is highly dependent on the concentration of oxygen (see e.g. [24,25]).

The realization that one can introduce metabolically responsive and relatively stable paramagnetic free radicals in the body prompted the introduction of another resonance technique (magnetic resonance imaging, MRI) in the field of redox research. At the beginning, nitroxides were studied as potential clinical contrast agents, primarily for tumors [26]. However, relaxation enhancement of nitroxides and corresponding contrast on MR images is around 10 times lower than with a standard MRI contrast agent (Gd-DTPA) per unit of concentration, so little further effort has been put along that line of research. However, with the advent of MRI machines for small animals numerous researches have been recently devoted to studying the redox state under different pathological conditions using nitroxides [27–31].

The main scope of this review is to cover research where the pharmacokinetics of nitroxides has been studied with a goal to investigate redox processes in normal and pathological conditions. The emphasis is on results obtained using EPR techniques, but examples from MRI studies are given when the focus of the study is on the pharmacokinetics of nitroxides and not just imaging using nitroxides as contrast agents. Particular attention is given to how fruitful a combination of EPR and MRI can be in achieving optimal analysis of the investigated subject. Details on EPR imaging alone of the oxidative stress can be found in the recent review [32]. Perhaps the most powerful application of *in vivo* EPRI is measurement of oxygen (EPR oximetry), but this subject will not be covered *per se* in this review. EPR oximetry has been extensively and regularly reviewed [33–35] and oximetry will be considered only when directly connected with the pharmacokinetics of nitroxides. The purpose of this review is not only to summarize results obtained so far but also to point to certain flaws in conducted research and to indicate a possible direction for improvement and development.

2. Technical consideration of magnetic resonance spectroscopy/imaging *in vivo*

Both EPR and NMR are resonant techniques that record spin transitions when a system in the magnetic field is exposed to adequate (resonant) electromagnetic irradiation. Although there are few fundamental differences between the principles of electron and nuclear magnetic resonance, differences in physical properties of the resonant species (unpaired electrons *vs*. nuclei with net spin) lead to profound differences in applications and techniques that are used to record spectra. Perhaps the greatest differences arise because the gyromagnetic ratio of an unpaired electron is ~700 times larger than that of a proton, so the resonance frequency/magnetic field ratio for the electron is 28 GHz/T, *vs*. 42.5 MHz/T for the proton. In principle, EPR is more sensitive than NMR per net spin in the same magnetic field. In practice, however, the situation is different, especially in biological systems. Namely, standard EPR spectrometers operate at much higher frequencies and lower fields than conventional NMR spectrometers. A standard commercial EPR spectrometer operates at 9.5 GHz (X-band) - 0.34 T; while NMR spectrometers operate at frequencies above 500 MHz, i.e. at magnetic fields above 10 T. Clinical MRI machines operate at fields at/or above 1.5 T while small animal imagers typically operate at 7 T or higher. The essential problem of EPR experiments on small animals is the non-resonant absorption of the electromagnetic radiation by the dielectric liquid water in biological systems. At 9.5 GHz this effectively limits the sample size to a thickness of a mouse tail. One could increase the penetration depth of microwaves into larger aqueous samples by increasing microwave power, but that would produce unacceptable heating of the subject (a microwave oven). Hence, animals can be studied only by reducing the operating frequency and corresponding magnetic field, but this results in reduced sensitivity. Studies on small animals have been performed at the S-band (2–3 GHz) with skin depth penetration, L-band (1.2 GHz) or even lower (700 or 280 MHz) for whole body imaging. Another problem is that commercial EPRI machines suitable for *in vivo* applications were not available until recently, hence most of the researchers used (and still are) a homemade apparatus or modifications of commercial ones.

The most important difference between *in vivo* MRI and EPRI is in the species that they detect. Both direct observations and theoretical calculations show that endogenous paramagnetic species such as paramagnetic metal ions and free radicals are present in insufficient concentrations to be detected directly by EPR *in vivo*. This presents an obvious problem since the paramagnetic substance has to be introduced in EPR experiments. On the other hand, this has some beneficial aspects, since the only paramagnetic species that will be observed *in vivo* will be those introduced by the experimenter. Also, the behavior of introduced nitroxides can be related to metabolism. MRI sees water protons which are abundant, enabling excellent images (water is 55 M and nitroxides are usually injected at doses around 1 mmol/kg of body weight). Nitroxides are seen indirectly through their effect on the relaxation of water protons. EPRI does not provide images of anatomy; it just shows the distribution of injected nitroxide within the body and does not have very good spatial resolution. Conversely, MRI has excellent spatial resolution and provides detailed anatomical information, but gives little information on the paramagnetic species involved. Both techniques have their advantages and drawbacks in *in vivo* ROS detection/imaging, thus the sensible simultaneous use of both is a way to employ the optimal potential of these techniques.

For example, it is possible to use both techniques in imaging modality and overlay EPRI providing redox information on top of MRI providing anatomical information [36,37]. There were also constructions of dual EPR/MR imaging machines where both types of information can be obtained without moving the animal [30,38,39]. Probably the best way to fuse EPR and MRI into a single machine is to use dynamic nuclear polarization (DNP or Overhauser effect, OMRI) which uses a unique method for detection of

radicals [40]. Briefly, the two-spin system (e.g. nitroxide/water protons) in the magnetic field is irradiated by RF at an EPR frequency of nitroxides (unpaired electron), magnetization is transferred to protons enhancing water proton NMR signal intensities and the overall effect is detected by conventional proton MRI. This effect is completely different from classical enhancement of proton relaxation by nitroxides (theoretically 330 times higher). Several studies have demonstrated the efficiency of this technique in both redox and oximetry studies [41–43]. It has been successfully demonstrated that OMRI machines accommodating large subjects including humans can be built [41,44] opening possibilities of combining all MRI capabilities with molecular specificity of EPR in diagnosis and treatment follow up clinical studies. However, these machines have to be homemade which is both technically demanding and expensive so only a few of them are in use. More detail on the technical aspects of the combination of magnetic resonance techniques can be found in recent reviews [45,46].

As emphasized before, the production of ROS species *in vivo* is rather low and they are short-lived, hence their direct detection is impracticable, if not impossible. Therefore, an addition of exogenous stable radicals such as nitroxides is needed to probe the redox state *in vivo*. An alternative is to use spin-traps which convert short-lived radicals (life-time shorter than milliseconds) into more stable ones (life-time tens of minutes). In both approaches there is a disruption of the natural redox system which raises the question of toxicity. Intravenous (*i.v.*) injection of nitroxides at the dose of up to 2 mmol/kg has been used to achieve reasonable signal-to-noise (*S*/*N*) ratio for EPRI or EPRS, although much lower doses have been used in the majority of studies. This is way beyond LD_{50} for nitroxides which is above 20 mmol/kg [47]. Transitory changes in blood pressure or animal twitches may occasionally occur especially when nitroxides with high cell penetrability are used. The situation is different when spin traps are used. Spin trapping is a very useful tool for studying a biochemical system *in vitro*, with some potential for *in vivo* applications [48,49]. Naturally occurring free radicals are scarce so a large amount of spin trap has to be added (toxicity is an issue then), trapped radicals are short-lived and have rather complicated EPR spectra which effectively prevents the use of EPRI. Spin-traps can be used *in vivo* for identifying free radicals produced by some process or agent (e.g. radiation), but are not very useful in pharmacokinetic studies.

There is a significant difference in the data collection procedure between EPRS and EPRI. A single field scan of a few tens of seconds is usually sufficient for the line intensity of nitroxide spectra to be measured (see Fig. 1A) and obtain a single time point. On the other hand, to obtain an EPR image it is necessary to collect more than 10 spectra recorded at different directions of the magnetic field gradient, which can turn out to be a lengthy procedure.

Early *in vivo* EPRI were rather crude (same as first MRI) and it took some 5–6 min to make 2D images using filtered back-projection with only 8 projections resulting in low spatial resolution and poor time resolution for pharmacokinetic studies [16,21]. Yet, at the same time the pharmacokinetics of nitroxides injected in mice has been studied with EPRS with less than a minute time resolution (Fig. 2A) [14]. It took a full 45 min to obtain a complete 3D data set [19], which certainly doesn't allow any temporal studies. Nevertheless, such studies have stimulated further development and today's machines are capable of producing 3D EPR images in around 1–2 min with up to 80 projections, where the actual performance depends on a selected task [50,51]. However, such machines are scarce and even such short imaging time may not be sufficiently fast to follow the reduction of some nitroxides. Hence the prudent choice of modality (EPRS or EPRI) is essential in conducting a proper experiment since there is always a tradeoff between spatial and temporal resolution. For example, it is reasonable to select EPRI for the brain studies since various parts of the brain or even different hemispheres might show a different reduction kinetic. It does not make much sense to use EPRI for studying e.g. the liver *per se* since it is unlikely that different liver lobes will show any difference in reduction capacity. Whole body imaging is justified if studying of multiple organs is attempted to simultaneously analyze the biodistribution of nitroxides. The situation is of course different when tumors are implanted in various organs where imaging is necessary not only to differentiate healthy tissue from tumors, but also to distinguish different zones within the tumor itself (see Section 5 for details). No spectroscopy/imaging dilemma is present when MR is used since nitroxides are detected only indirectly through imaging. Most MRI machines are capable of generating images with sufficient anatomical resolution in tens of seconds. However, such imaging sequences usually do not have good sensitivity in detecting the effect of nitroxides.

3. Biochemistry of nitroxides

Cyclic aminoxyl radicals with tetraalkyl substituents flanking the $>N–O^{\bullet}$ functionality are most often used as probes for the redox status *in vivo*, especially derivatives of TEMPO #**1** or PROXYL radicals #**9** (Scheme 1). In contrast to nitroxide adducts derived from nitrone spin traps, these probes persist almost indefinitely in

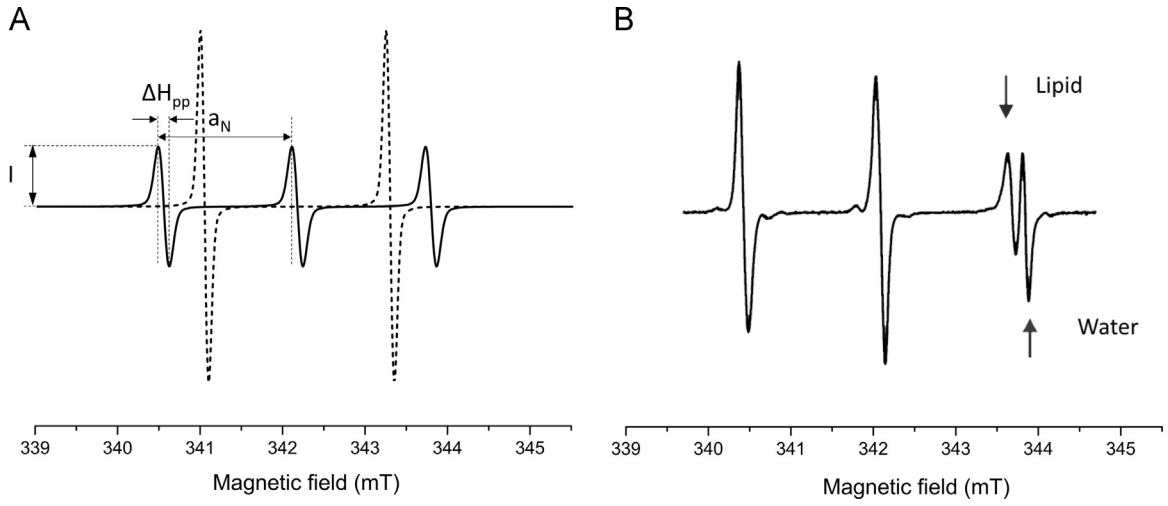

Fig. 1. A. EPR spectrum of freely rotating nitroxide (TEMPONE #**4**) in an aqueous environment. *I* – peak intensity, a_N – hyperfine splitting, ΔH_{pp} – line width. The inserted spectrum (dotted line) is ^{15}N substituted and perdeuterated TEMPONE (^{15}N PDT). B. EPR spectrum of TEMPO #**1** in the nonpolar (hydrocarbon) and polar (water) mixture.

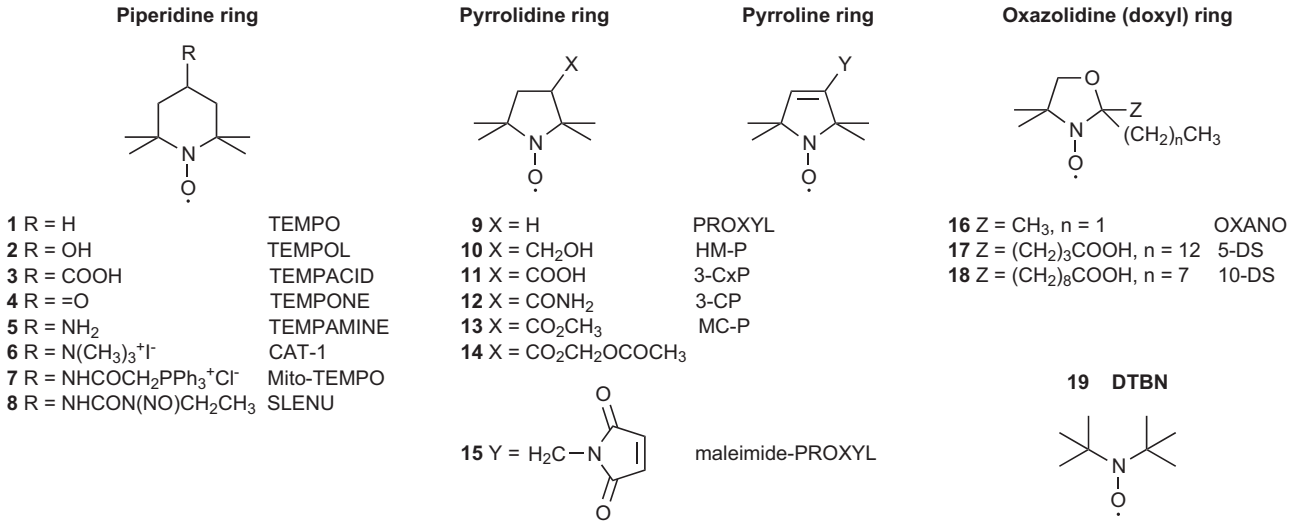

Scheme 1. Characteristic aminoxyl radicals used as probes of the redox status. These compounds are more frequently referred to as "nitroxides" or "nitroxyl radicals", despite IUPAC recommendations. Most studies were conducted with derivatives of TEMPO 2,2,6,6-tetramethylpiperidine 1-oxyl (#**1**) and PROXYL 2,2,5,5-tetramethylpyrrolidine 1-oxyl (#**9**). Lipophilic doxyl stearates are incorporated into the membrane in cells with the doxyl moiety either close to the surface membrane in #**17** or deep in the membrane in **#18** .

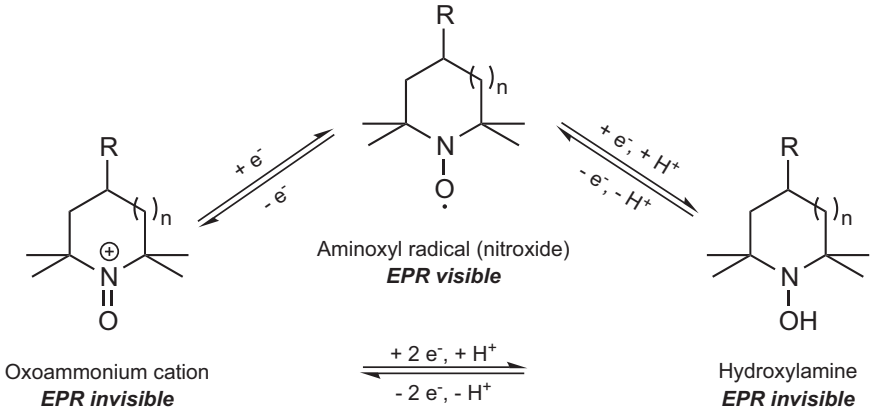

Scheme 2. Redox species associated with aminoxyl (nitroxide) radicals ($n=0$ or 1, pyrrolidine or piperidine).

a buffered solution due to an exhaustive substitution at the α-position to the nitrogen and are dubbed as stable free radicals.

A typical spectrum of nitroxide is presented in Fig. 1A. All piperidine or pyrrolidine nitroxides listed in Scheme 1 will have almost identical spectra. Side groups do not contribute to the overall appearance of the EPR spectrum, except through changes of rotational time which may have an effect on the line width (ΔH_{pp}). Multiple lines (line splitting) in EPR spectra originate from the so-called hyperfine interaction of the unpaired electron spin with the nuclear spin of ^{14}N ($I=1$) which according to the quantum mechanical rule determines the number of lines (number of lines $= 2I+1$). A spectrum of ^{15}N-PDT has only two lines since the nuclear spin of ^{15}N is $I=1/2$. Perdeuteration removes super-hyperfine line broadening caused by interaction of the electron with neighboring protons (nuclear spin of deuterium is one) and the overall effect is that the line height of ^{15}N-PDT is higher than in natural nitroxides containing ^{14}N resulting in a 5-fold increase of the signal-to-noise ratio. The benefits for EPRI are well understood and explained [10] and ^{15}N-PDT has been used in several studies [52,53] but the wider use of ^{15}N substituted and perdeuterated nitroxides has been somewhat limited by their relatively high price, which becomes an issue when *in vivo* experiments need to be performed and relatively large amounts of nitroxides have to be injected.

The hyperfine splitting of nitroxides depends on the polarity of the solvent (Fig. 1B). In a nonpolar solvent the unpaired electron delocalizes from the nitrogen atom, so the hyperfine coupling is decreased when compared to the aqueous solution. This is an important feature signifying that nitroxides can report on their environment and a number of nitroxides reporting on micropolarity, microviscosity, local pH, temperature etc. have been developed. On the other hand, the amount of nitroxide *in vivo* is always determined from the intensity of the low- and/or mid-field peak since the high-field peak is not reliable for such measurements. The doxyl stearate (DS) nitroxides are almost exclusively located in phospholipid membranes, but their spectra are complicated due to unresolved hyperfine splitting and are seldom used in *in vivo* studies, but are very useful for studying biochemical mechanisms *in vitro*.

These "stable" radicals can, however, participate in redox reactions with biological compounds or enzymes and thus report on the redox status of the cell by shuttling between three forms shown in Scheme 2). Since the position of the equilibrium reflects the redox status, hydroxylamines or acyl-protected hydroxylamines, which are converted to hydroxylamines by esterases in cells and tissues, can be used as alternative probes for oxidative

stress [54].

After incubation of a nitroxide radical with cells, a decay of the EPR signal is observed, mainly due to the net reduction to hydroxylamine [55,56]. Many studies (mainly dating back to the 1970s and 1980s) investigated the mechanisms underlying EPR signal decay of nitroxides using various models or integrated systems and the general principles of nitroxide metabolism are now well understood. Several mechanisms are involved, the relative importance of which varies depending on the subcellular localization of the nitroxide, hence on its lipophilicity and charge, and also on the tissue of interest [57]. The rate of reduction of nitroxides by ascorbic acid, a standard screening test for nitroxide stability, is mainly dependent on the type of ring system [58–60]. Nitroxides based on a six-membered piperidine ring are generally reduced faster than analogues based on a five-membered pyrrolidine ring (Scheme 1). The flexibility of the piperidine ring, facilitating access of ascorbate to the nitroxide, appears to be a better explanation for this effect than the difference in redox potentials [60]. The presence of a double bond in the five-membered structure slightly enhances susceptibility to reduction. Ring substituents in each series further influence the reaction rate, though to a lesser extent. Anionic compounds (such as #**3**) are more stable than neutral compounds (like #**2** or #**4**), which in turn are more stable than cationic nitroxides (such as amine #**5** or tetraalkylammonium ion #**6**). This is consistent with an electrostatic interaction between the nitroxide and the monoanion ascorbate [58].

In functional biological systems, reduction of the nitroxides occurs mainly within cells [24,61], so that the main structural criterion governing the rate of reduction appears to be the ability to enter cells. Charged compounds such as CAT-1 #**6** or 3-CxP #**11** are virtually incapable of crossing phospholipid membranes and are fairly resistant to reduction [24]. Once within the cell, the rate of reduction of the nitroxide is largely dependent on the ring size, piperidine derivatives being reduced faster [24,61]. In cell suspensions, the reduction process is mainly enzyme-dependent. It may take place in mitochondria, especially mediated by ubiquinol in the electron transport chain [62,63]. NAD(P)H-dependent systems in microsomal fractions can also be involved in the reduction [59,64]. Alternatively, soluble enzymes of the hexose monophosphate shunt can influence the reduction [65]. However, cytosol demonstrates low reducing activity, except in cells containing large amounts of ascorbate like hepatocytes and kidney cells [64,66]. Thiols do not significantly reduce the nitroxide radical *in vitro*. However, they can indirectly contribute to its reduction in biological systems by acting as secondary sources of reducing equivalents [67]. Increased concentrations of oxygen within cells usually lower the reduction rates by changing the redox states of mitochondrial enzymes involved. The extent of this effect varies depending on both the cell type and the lipophilicity of the nitroxide [24,62,65,68,69]. The rate of reduction of lipophilic nitroxides #**17** and #**18** in the doxyl stearate series is especially sensitive to severe hypoxia (intracellular $[O_2] < 1\ \mu M$) [62,68,69]. In the presence of oxygen, oxidation back to the nitroxide of the lipid soluble hydroxylamines occurs in membranes at the level of cytochrome *c* oxidase and competes with the reduction of nitroxides at a rate that increases with oxygen concentration [70]. In contrast, water-soluble hydroxylamines are not significantly oxidized by cells [70].

In the context of oxidative stress, the nitroxide can be oxidized to the oxoammonium cation by various oxidants such as the ferryl heme species [71,72], $HO_2^{\bullet}$ [73–75], $^{\bullet}NO_2$, and $CO_3^{\bullet-}$ [75–77] with rate constants around 10^6–$10^8\ M^{-1}\ s^{-1}$. Direct reaction with the hydroxyl radical does not seem to be significant [78]. Instead, nitroxides are known to detoxify $HO^{\bullet}$-derived secondary radicals such as protein-based and alkylperoxyl radicals [79,80]. These reactions lead to an increased decay of the EPR signal compared to normal tissues. The oxoammonium cation is a strong oxidant and potentially harmful if it were to react with cellular components [81,82]. However, it can be recycled to the nitroxide by a reaction with $O_2^{\bullet-}$ at diffusion-controlled rates, the nitroxide/oxoammonium pair acting as an SOD-mimic [73]. Alternatively, the oxoammonium cation seems to be efficiently reduced to hydroxylamine by two-electron donors such as NAD(P)H or thiols [74]. The comproportionation reaction between the oxoammonium cation and the hydroxylamine occurs at a negligible rate and does not contribute to recycling of the nitroxide in cells [81]. Being an efficient chain-breaking antioxidant in the Fenton reaction, the nitroxide also decays through its interaction with reduced transition metal ions (Fe^{II}, Cu^{I}), yielding the hydroxylamine [83]. The latter can in turn be oxidized by a variety of reactive oxygen species ($O_2^{\bullet-}$, $HO^{\bullet}$, $ONOO^-$, H_2O_2 in the presence of transition metal ions), the reaction with $O_2^{\bullet-}$ being the primary non-enzymatic recycling pathway, though at a rate lower by several orders of magnitude than the rate of the reaction of $O_2^{\bullet-}$ with nitroxide [78, 84].

4. Analysis of pharmacokinetic curves

Previous Sections were devoted to various chemicals and machines needed to obtain the proper pharmacokinetical curve of nitroxides. However, even having a perfect pharmacokinetic curve, there are still obstacles before we can reach a conclusion on the redox status (processes). Namely, the signal decay rate which should reflect redox processes in the selected organ depends on, beside the reduction of nitroxides, also on several kinetic factors such as the distribution of the spin probe from the blood to the tissue and within different tissue compartments, urinary excretion through kidneys, fecal excretion through liver and bile, etc. To illustrate the complexity of the problem, several examples of pharmacokinetic curves for the two most studied organs (brain and liver) and a few commonly used nitroxides are given in Fig. 2.

Fig. 2A presents the first *in vivo* measurement of the pharmacokinetics of different nitroxides in the liver region obtained at the L-band with a surface coil [14], which has been closely followed by similar studies [15,17]. Different kinetics can be explained by the difference in the structure of these nitroxides (see Section 2). TEMPOL is a piperidine ring nitroxide (#**2**, Scheme 1) and the side group enables its high cell membrane permeability. Hence, the fast signal decay is to be expected mostly due to the whole body intracellular reduction of TEMPOL to hydroxylamine. The CAT-1 is also a piperidine ring nitroxide (#**6**), but its charge prevents permeation to cells and intracellular reduction. It appears that the signal decay of CAT-1 is essentially due to kidney elimination since there was a concomitant increase of CAT-1 in the bladder where it was subsequently reduced by ascorbate present in urine. The 3-CxP is pyrrolidine nitroxide (#**11**) to which cell membranes are reportedly impermeable just like for CAT-1, yet the difference in the decay pattern is obvious. No attempts have been made to explain this bi-exponential behavior by authors, but the same signal decay pattern has been found in a subsequent publication using EPRS and 3-CxP [15,17], contrary to the data obtained using EPRI [16,21,88], but the latter did not have a good time resolution to properly assess the signal decay.

The research has been accelerated by synthesis of a new class of nitroxides aimed primarily for brain studies. These blood-brain-barrier (BBB) permeable nitroxides [89–92] improved brain research, but also became very popular in studying other organs, especially BBB and cell permeable 3-CP (#**12**) nitroxide. Fig. 2B and C show results obtained for the pharmacokinetics of several nitroxides in liver and brain compiled from various sources. The time course curves for the decay of 3-CP in various studies differ, which is only to be expected –

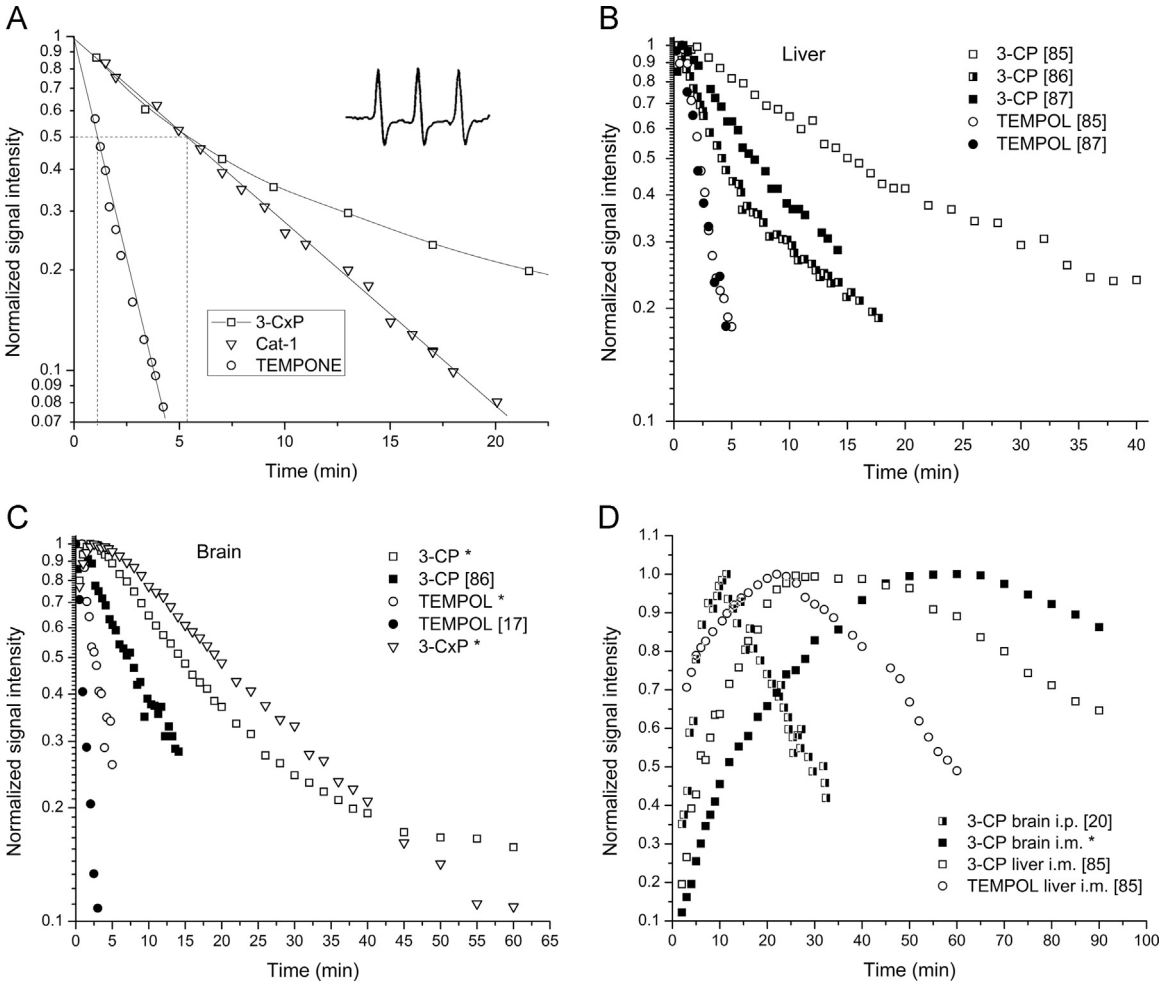

Fig. 2. *In vivo* pharmacokinetics of nitroxides. A. Normalized decrease of the EPR signal intensities of nitroxides from the liver region of mice following the injection of three different nitroxides at doses of 0.10 - 0.15 mmol/kg. Dotted lines denote the time of signal decrease to the half of the original value (half-time, $t_{1/2}$). Inserted is an *in vivo* EPR spectrum of 3-CxP, **#11** (called PCA at the time) obtained 5 min after injection demonstrating an excellent signal/noise ratio (adapted from [14]). B. Compilation of pharmacokinetic data for two nitroxides in the liver (tail vein injection). C. Compilation of pharmacokinetic data for three nitroxides in the brain (tail vein injection). D. Compilation of pharmacokinetic data for three nitroxides in the liver and brain *(i.m.* or *i.p.* injection). Sources are given in brackets. Asterisks in C–D denotes some unpublished data from authors [85].

different animals (rat or mice) on a different diet were used, different doses of nitroxides, temperature control, ascorbate content, etc, but they are not single exponential (decay after initial increase is what reflects the redox state). We deliberately selected examples to demonstrate the point, but this behavior has been found in the majority of studies, yet authors treated those, with a few exceptions [86,90], as the pseudo-first order kinetics deriving kinetic parameters from the initial slope. The decay of TEMPOL and similar nitroxides appears to be single-exponential in both liver and brain, the feature which has been found in all studies. Nevertheless, it is difficult to believe that a nitroxide that readily distributes into various organs has such a simple overall pharmacokinetics; we simply do not have sufficiently fast machines to study it with adequate time resolution and sensitivity to reveal the true pharmacokinetics.

Fig. 2A illustrates how misleading treating all decay curves with pseudo-first order, i.e. with a single $t_{1/2}$ can be. CAT-1 and 3-CxP have the same $t_{1/2}$ and very different overall pharmacokinetics. Regardless of whether the decay curve appears to be single exponential, *in vivo* pharmacokinetics of nitroxides in organs certainly does not fit to a single compartment model. The EPR signal of nitroxides as measured in a certain organ is inevitably composed of signals coming from the blood and that organ. Further, tissues are composed of various compartments with a different reducing capacity.

Hence the primary goal in careful analysis of the pharmacokinetics of a certain nitroxide should be to distinguish the signal decay arising from the reduction of a nitroxide within the organ (extravascular/extracellular space and cells) from elimination (washout) and/or reduction in the blood itself. To do that pharmacokinetic models are needed for analysis of decay curves, which then requires performing a multiparametric fit. To verify the outcome, it is necessary to have data from independent measurements of certain kinetic parameters. Unfortunately, even measurements of the reduction of nitroxides in blood *in vivo* proved not to be an easy task. Numerous studies have been performed to measure reduction of nitroxides in fresh blood *in vitro* or in the tail (e.g. [22,27,93–96]). Data obtained from these measurements are useful, but both approaches have serious flaws. *In vitro* measurements of reduction of nitroxide in blood give information on reducing capacity of the blood itself (usually very low), but in an *in vivo* experiment the blood nitroxide signal measured in a given organ is actually reporting events from the whole body. Measurements of nitroxide decay in the tail are hampered by the fact that nitroxides can be distributed in tissues other than blood [22] thus the measured decay is composed of processes in both tissues. Measurements of the nitroxide concentration in the circulating blood have been performed by a surgical procedure by which the jugular vein was cannulated and blood was via tube circulated

through the X-band cavity [96,97]; a procedure that gives reliable results, but is technically demanding. MRI measurements of the pharmacokinetics of nitroxides in the blood *in vivo* have been performed [28,98,99], but MRI is measuring nitroxides indirectly and the procedure is not quantitative.

Another way to uncouple tissue reduction from the washout is to use *i.v.* injection of KCl at the peak of the concentration-time curve which produces almost immediate cardiac arrest [27], so that the further signal decay is only due to nitroxide reduction within the tissue. Also, a possibility of gaining insight into decay mechanisms is to perform simultaneous studies on the same animal model but using nitroxides with different characteristics (cell permeability, resistance to reduction, lipophilicity). The approach is illustrated in Fig. 2C where it is obvious that two nitroxides, 3-CP and 3-CxP, have different decay kinetics due to different cell-permeability. Similar experiments have been performed in a rodent brain [90,95] and tumor [98], but no pharmacokinetic models were used to analyze results and assess the role of different structures in the overall reduction decay. On the whole, there is no study where all these possibilities have been employed together to perform the detailed analysis of nitroxide pharmacokinetics.

Reduction of nitroxides when intramuscular (*i.m.*) or intraperitoneal (*i.p.*) injection is applied shows a completely different situation (Fig. 2D). Now the dominant feature is the time for nitroxides to reach the organ and not so the reduction kinetics afterwards. Again the reduction of the TEMPOL signal is much faster than for 3-CP, but it should be noted that the signal persisted for almost an hour, unlike for *i.v.* injection, which is consistent with similar previous studies [93,100]. Also, the study of hydroxylamine showed the same basic difference in pharmacokinetics between the *i.v.* and *i.p.* injection [101]. These routes of administration are not so useful for pharmacokinetic studies and are rather difficult to model. Nevertheless, it is possible to obtain data on perfusion, oxygenation and tissue viability by combining *in vivo* EPR and MRI and using the proper pharmacokinetic model. It is somewhat puzzling that many authors just did not pay much attention to the route of administration when discussing their results and comparing kinetic data from different administration routes. Almost all examples given here are from *i.v.* injections of nitroxides unless stated otherwise.

5. Selected examples

The EPR and MRI techniques have been employed to map the distribution of free radical metabolism in a variety of organs and tissues. The list of examples and references given below is by no means exhaustive; characteristic examples are selected to illustrate capabilities of these techniques to *in vivo* investigate the redox status, focusing on the disease associated alterations of it.

5.1. Skin

The skin is an ideal target organ for EPRI for several reasons. It is thin and detection of nitroxides applied topically does not require large penetration depth of microwaves so one can use the S-band (2.2–3.0 MHz) for *in vivo* or even X-band for *in vitro* specimens, which results in an improved sensitivity. Imaging does not require full 2D or 3D imaging; once nitroxides are applied topically a simple spectral-spatial 1D imaging with one gradient orthogonal to the skin surface is sufficient to obtain distribution of nitroxides and the redox status in the different skin layers. The surface loop coils are sufficient, i.e. the whole objects need not to be within the resonator, which allows the EPRI of objects of any size, including humans. This is an important feature since it opens the possibilities of application of EPR in human (clinical) studies of not only

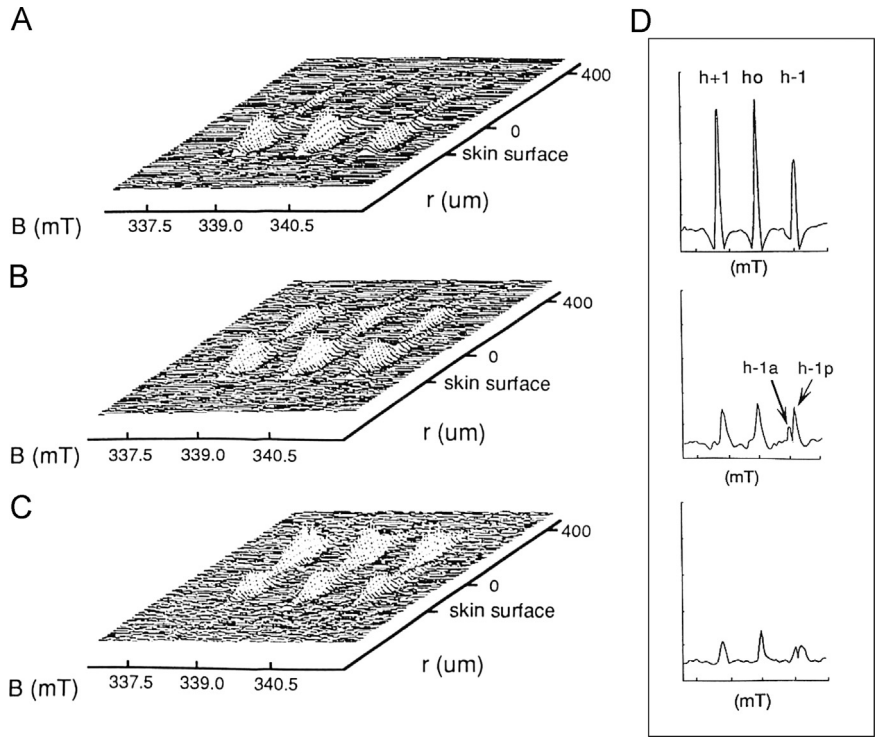

Fig. 3. Penetration of DTBN (di-*tert*-butylnitroxide #**19**, a small non-cyclic nitroxide) into mouse skin as monitored by X-band EPRI. A, B, C Images of time dependent changes of the distribution of DTBN obtained in the presence of a field gradient orthogonal to skin surface: A – 5 min; B – 15 min; C – 45 min. D. EPR spectra of DTBN (2nd harmonics) in different layers of the skin: top - epidermal surface; middle – epidermis; bottom – dermis. A splitting of the high field line, h-1, into two peaks indicates distribution of DTBN between apolar (h-1a) and polar (h-1p) microenvironments within the epidermis and dermis. Adapted from [105].

pharmacokinetics of nitroxides, but also of mechanism of action of certain drugs, skin melanoma, oximetry [102–104].

A nice illustration of pharmacokinetics of nitroxides in skin as studied by 1D spectral-spatial EPR is given in Fig. 3. Fuchs et al. [105] studied diffusion of several nitroxides into skin biopsies of hairless mice. By studying the spatially resolved diffusion of maleimide-PROXYL (#**15**) nitroxide into different skin layers (surface, epidermis, dermis), which chemically reacts with thiol groups, they effectively determined the spatial distribution of thiol groups as well. The analysis of spectral features showed spatially resolved partitioning of the nitroxide di-*tert*-butylnitroxide (DTBN) #**19** between polar and apolar regions (Fig. 3D, compare with Fig. 1B). They also found that penetration of lipophilic nitroxides is much faster than penetration of more hydrophilic nitroxides. They also studied percutaneous absorption and distribution of a nitroxide-labeled drug (estradiol) and a local anesthetic (procaine) finding that the former readily penetrates into deep skin layers while the latter does not, even in the presence of a penetration enhancer, such as dimethylsulfoxide. This paper clearly demonstrated that both the rate and spatial distribution of the physiological processes involved in the metabolism of nitroxides or nitroxide-labeled compounds can be studied.

Although this research has been performed using X-band EPR and skin biopsies, it set the stage for further extension for *in vivo* applications, which always raises the question of toxicity. Various nitroxide probes have been tested for biostability in the skin and possible cutaneous irritation [106,107]. The stability in skin biopsies, homogenates and cell cultures of keratinocytes decrease in the following order imidazoline > pyrrolidine > DTBN > piperidine > oxazolidine [106]. The irritation potency of different nitroxides has been classified as nonirritant to moderately irritant, thus, nitroxides can be safely employed for *in vivo* EPR studies of skin even at high concentrations (100 mM) [107].

The fact that some nitroxides and drugs are simply impermeable to skin, as demonstrated by studying their spin-labeled equivalents, prompted another line of research of investigating potential drug carriers. Group of authors [108,109] systematically studied potential applications of liposomes as drug carriers for topical treatment of skin disorders using 1D EPR. They found that entrapment in liposomes promotes the penetration of otherwise impenetrable charged nitroxides into skin and that the loss of integrity of liposomes in different layers of the skin (indicating the site of delivery) can be assessed. Studies revealed that the size and phospholipid composition of liposomes significantly influence their efficiency, thus providing the base for their application in medicine and cosmetics.

Nitroxide pharmacokinetics has been studied on various preparations of skin homogenates and cell cultures [106,110], animal [106,111,112] and human biopsies [106,113], as well as *in vivo* on animal models [53,111,112,114] or on human subjects [111,115]. The principle for measuring distribution and pharmacokinetics is the same as outlined in Fig. 3, except that measurements were performed *in vivo* at lower frequencies and using more sophisticated equipment (Fig. 4).

The larger part of research has been devoted to the evaluation of the UV irradiation influence on the redox status of skin. UV irradiation of the skin can cause inflammatory processes through several possible mechanisms: (1) direct damage of DNA; (2) generation of different free radicals (ROS, lipid derived radicals – peroxyl or alkyl), and (3) production of inflammatory agents (prostaglandines, histamine). EPR studies are of importance for two main reasons: (1) better understanding of processes underlying postulated oxidative damage induced by UV irradiation; (2) examining free radical scavenging efficacy of various antioxidants and sunscreens for protection.

Enhanced production of ROS following UV irradiation of the skin has been demonstrated by spin trapping [116,117] and also by analyzing nitroxide decay kinetics [53,111–113,115]. *In vivo* measurements of UVB influence on rat skin [53] and analysis of the obtained ^{15}N-PDT reduction kinetics showed the decrease of both penetration and reduction rate in all skin layers after the exposure to UVB light. The decrease of the reduction rate constants was more pronounced in dermis and hypodermis than in epidermis layer. Oximetry measurements showed that pO_2 did not change after treatment with UVB light, hence oxygen concentration and microcirculation were disqualified as possible causes of alterations in nitroxide reduction rates. Results of other authors [111–113], however, showed the opposite trend – the increase of reduction rate of nitroxide after the treatment of skin by UV light. Exposure of the skin not only led to the change in nitroxide signal decay rate constant, but also affected the shape of the kinetics curve (Fig. 5A) [113]. Namely, when three different nitroxides (TEMPO, 3-CP and 3-CxP) were topically applied to nonirradiated skin biopsies, kinetics corresponded to first order exponential process while upon irradiation by UV light all the kinetics could be fitted by bi-exponential function. It has been assumed that the faster process is due to reduction of nitroxides by radicals produced by UV irradiation, while the slower process corresponds to reduction of nitroxides by so called daughter radicals of ROS (for instance lipid carbon centered and lipid peroxyl radicals). The work of Takeshita et al. [112] adds to understanding of a probable causes of nitroxide

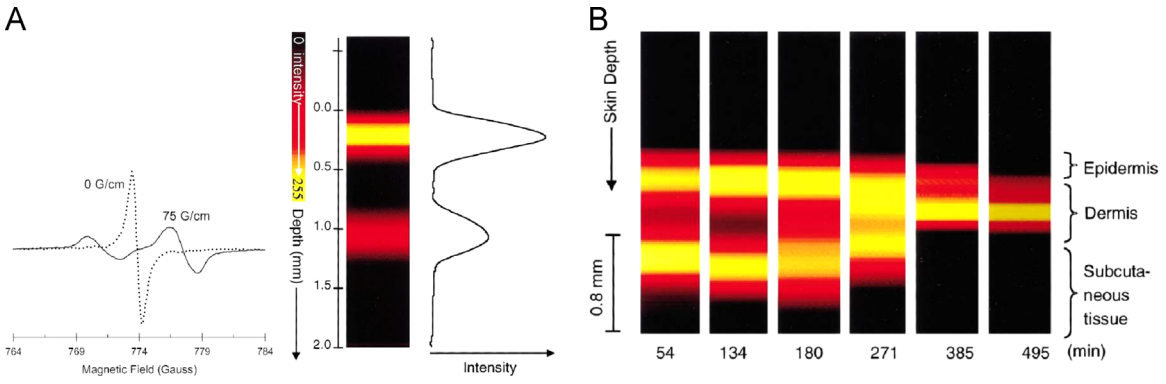

Fig. 4. S-band, 2.2 GHz, EPR spectroscopy and imaging of ^{15}N-PDT in phantom and skin *in vivo*. A. The low-field peak of the nitroxide doublet in a layered disc phantom scanned in the absence (0 G/cm, dotted line) and presence (75 G/cm, solid line) of field gradient applied normal to the surface of the disc phantom. The splitting observed in the presence of the field gradient is due to the spatial separation of the two discs in the phantom. 1D spatial image of disc phantom obtained from the projections. The data show that a spatial resolution of 0.1 mm can be obtained. B. Color-coded image of the time course of spatial distribution of ^{15}N-PDT applied to a skin of human forearm as a function of skin depth. The decay kinetic has been fitted to a single-exponential. Adapted from [115]. (For interpretation of the references to color in this figure legend, the reader is referred to the web version of this article)

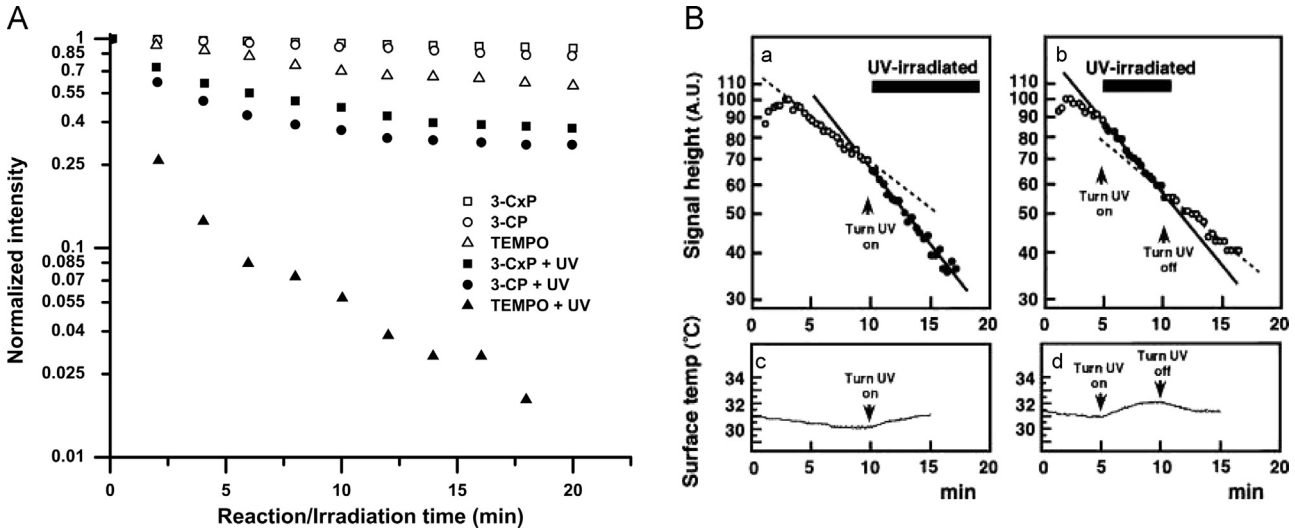

Fig. 5. Kinetics of nitroxide reduction and UV irradiation. A. Reduction of the nitroxides 3-CxP, 3-CP, and TEMPO applied to skin biopsies incubated in a 0.1 mM water/ethanol solution of the nitroxide for 5 min. The reduction curves represent the signal loss without (open symbols) and with UV irradiation (closed symbols). Adapted from [113]. B. Pharmacokinetics of nitroxide (3-CP) as measured with L-band EPR and surface coil placed on dorsal skin of a nude mice after *i.v.* injection of 3-CP [112]. Distinct rapid and reversible changes in decay rate of 3-CP EPR signal in response to starting and stopping UVA+B illumination are clearly observable (a, b). The response of skin surface temperature to the turning on and off of the UV light shows minor changes (c, d), which cannot affect nitroxide reduction.

signal decay in the skin of living mice exposed to UVA+B light. First, results clearly demonstrate that UV irradiation enhances reduction of nitroxides (Fig. 5B). Preadministration of ROO• scavengers to the mice diminished rate of 3-CP signal decay in irradiated mice, whereas HO• scavengers had no effect. None of the previously mentioned scavengers affected 3-CP signal decay in nonirradiated mice. Such finding indicated that faster loss of EPR signal in skin exposed to UVA+B light occurred due to enhanced ROS production, more specifically of ROO• radicals.

5.2. Brain

The brain has been the subject of numerous ROS studies using EPR/MRI. These include the studying of various conditions that can induce oxidative stress and alter redox status such as ageing and isolation, various induced diseases, hypoxia. Due to brain complex structure most studies used an imaging mode often combining EPR and MRI, which sometimes resulted in a low time resolution.

The role of ROS and antioxidants on ageing is the subject of ongoing research and EPRS studies on young and old rodents revealed that ageing diminishes the ability of the brain to reduce injected nitroxides [20,86]. The study on intracerebral reducing ability after acute stress in adult rats showed diminished reducing ability in rats that were subjected to neonatal isolation [118].

Transient middle cerebral artery occlusion (MCAO) is a common method in studying ischemia/reperfusion (I/R) injuries. The *in vivo* generation of ROS and its location in the brain were analyzed from the EPR signal decay data of three intra-arterially injected spin probes with different membrane permeability (Fig. 6A). The EPR signal decay of the probe with intermediate permeability was significantly enhanced 30 min after reperfusion following MCAO, whereas no enhancement was observed with the other probes. The antioxidant MCI-186 completely suppressed the enhanced *in vivo* signal decay after transient MCAO. These results demonstrated that ROS generated during the initial stages of transient MCAO cause brain injury. On the other hand, reduction rates of MC-P (#**13**) were significantly decreased 3h after reperfusion following transient MCAO [27]. A combination of 3D EPRI and MRI has been used to map the half-lives of HM-P (#**10**) in the mice brain 24h after MCAO [51]. Inhomogeneous half-lives were clearly mapped pixel-by-pixel in the infarcted hemisphere (Fig. 6B) and the average half-life of nitroxide was about 20% longer when compared to the unaffected hemisphere. It has been concluded that the difference arises from the different amount of ascorbate in tissues.

A study of intracerebral reducing ability has been performed on

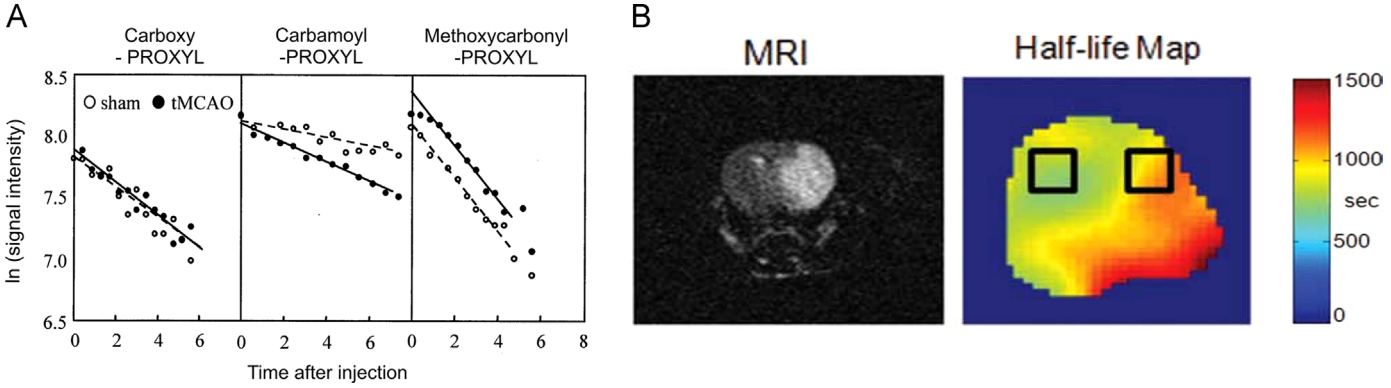

Fig. 6. Reduction of nitroxides in ischemia reperfusion models. A. The decay kinetics of different spin probes (3-CxP, 3-CP, MC-P) administered intra-arterially to rats after 30 min of reperfusion, after 1 h of MCAO [95]. B. Images of the brain 24 h after MCAO. The MRI T2W image shows a massive lesion in the infarcted hemisphere, while the half-life map shows the difference in nitroxide reduction. The selected regions of interest ROIs were used to calculate average reduction half-times [51].

the rat model of neonatal (7 day old) hypoxic-ischemic encephalopathy [119]. The ability of a mature rat brain to reduce BBB permeable HM-P (#**10**) was depleted when compared to the control; however this depletion was diminished by administering an antioxidant agent after a hypoxic-ischemic insult.

Fig. 7 illustrates the basic concept of time resolved brain EPRI [120]. Rats treated with kainic-acid (KA) induced seizure showed that the hippocampal half-life of nitroxide MC-P (#**13**) after seizures was significantly prolonged indicating impaired reducing ability, whereas the prolongation of the cortical half-life was not significant. The authors ascribed this difference to the different amount of ascorbate in those tissues. These findings were confirmed by using an acyl-protected hydroxylamine which undergoes intracellular oxidation to nitroxides [121] showing that oxidative stress in the hippocampus and striatum in KA-treated animals is enhanced, but not in the cortex.

A common way of altering the redox state is to induce sepsis using lipopolysaccharide (LPS). Fig. 8A shows that reduction of HM-P in the brain of LPS treated mice is much faster than in the control and images showed that the LPS-induced effect is homogeneous in all brain tissues [122]. The reduction rates were slower than those in septic mice and became closer to the control when aminoguanidine or allopurinol, which inhibit enzymatic activities of induced nitric oxide synthase and xanthine oxidase, respectively, were applied.

The reduction of nitroxide mito-TEMPO (#**7**, BBB- and cell-penetrating) has been studied in the Parkinson's disease animal model (MPTP-treatment) in mice using MRI (Fig. 8B) [31]. The fast reduction ($t_{1/2}$ around 40 s) of mito-TEMPO has been recorded in the dopaminergic area of the normal brain while in the MPTP treated mice the mito-TEMPO enhanced MRI signal persisted much longer ($t_{1/2}$ around 20 min). Based on the redox cycle of mito-TEMPO, the authors concluded that superoxide is a major inducer and/or mediator of neurodegenerative damage in Parkinson's disease.

A couple of studies performed on the effect of various neuroleptics, known to induce oxidative stress, on the brain redox status revealed diminished ability of various brain areas in treated animals to reduce the injected nitroxide [123,124].

5.3. Other organs

Numerous model diseases and harmful conditions have been studied using reduction of nitroxides. At the beginning measurements were performed by placing surface coils over the selected organ or inserting a certain part of the body into the loop coil. Application of whole body EPRI was rare due to poor spatial resolution, but this has changed with the development of EPR machines. Nowadays, whole body imaging is more frequently performed using some type of combining EPR with MRI (imaging fusion or hybrid imagers, see Fig. 9) [30,36,37]. Numerous useful studies have been performed on isolated perfused organs, particularly on the heart [125], but here only *in vivo* studies will be reviewed.

Lungs have been studied mostly to determine the effect of various toxins on their redox status [30,126–128]. An early EPR study of nitroxide (administered intratracheally after euthanasia) reduction in lungs revealed the well-known pattern that TEMPO derivatives are reduced much faster than 3-CP, while 3-CxP was almost not reduced at all [129]. An *in vivo* study on mice after intratracheal instillation of diesel exhaust particles (DEP) showed that such treatment significantly enhances the decay rate of CAT-1 [127]. The enhancement was completely suppressed by the administration of $HO^{\bullet}$ scavengers (catalase or desferrioxamine) showing the direct evidence of $HO^{\bullet}$ generation by DEP. These findings have been corroborated by another study where it was found that reduction of CAT-1 in DEP mice and lung injury were suppressed by a thiol protein thioredoxin-1 [128]. The reduction of TEMPOL in lungs of asbestos exposed mice was significantly decreased during the acute disease progression indicating changes in the lung redox status in acute asbestosis [126]. It has been found [30] that mice exposed to second hand smoking have a diminished ability to reduce nitroxides not only in lungs but also in almost all other organs (Fig. 9).

A number of studies have shown that oxidative stress is increased in diabetes which via free radicals contributes significantly to the pathogenesis of diabetic angiopathy. Extensive research has been performed by a Japanese group [87,130–133] using streptozotocin-induced diabetes in rodents and reduction of 3-CP to study source(s) of stress as well as agents that can be potentially used in antioxidative therapy in diabetes. The reduction of nitroxides in both liver and kidneys was faster in diabetes than in the control in all studies. One of the main conclusions is that vascular NAD(P)H is the principal contributor in diabetes induced oxidative stress, which has been confirmed by the findings that it is suppressed by administering SOD, apocynin (NAD(P)H oxidase inhibitor), or statin.

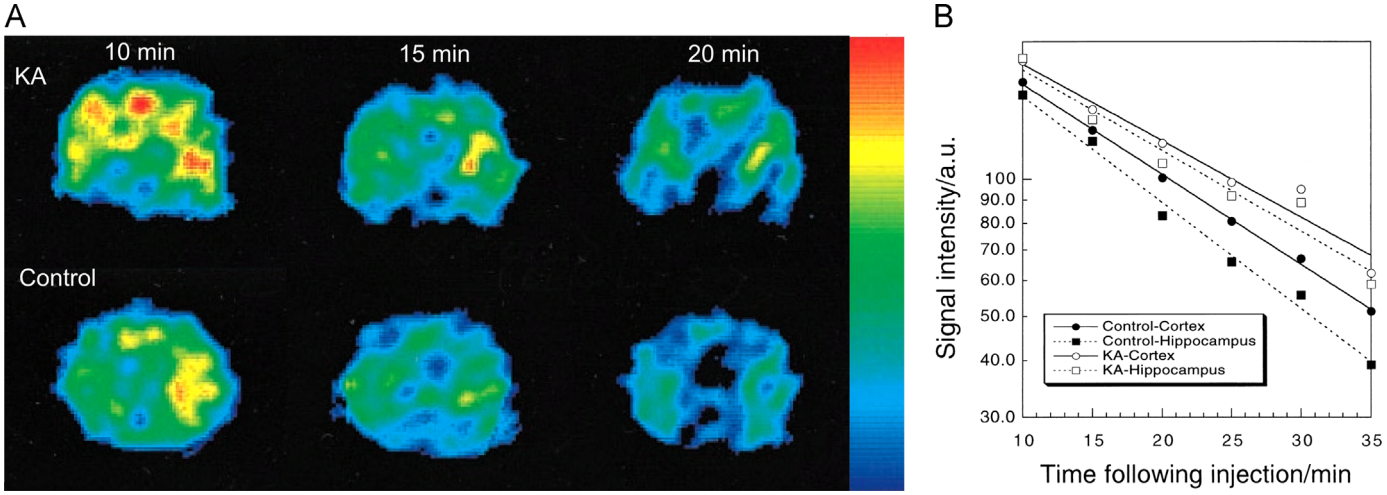

Fig. 7. EPRI of the rat brain in induced seizure. A. The dynamic pattern of selected transversal EPR images of the rat head 5 mm posterior to the bregma in the KA-treated and control groups at different times following injection of nitroxide MC-P (#**13**). B. Pharmacokinetic curves for brain regions. The cortical half-lives of MC-P in the control and KA groups were 18.0 ± 1.2 and 19.2 ± 0.7 min, while the hippocampal half-lives of MC-P in the control and KA groups were 10.4 ± 0.8 and 15.9 ± 0.7 min, respectively. Adapted from [120].

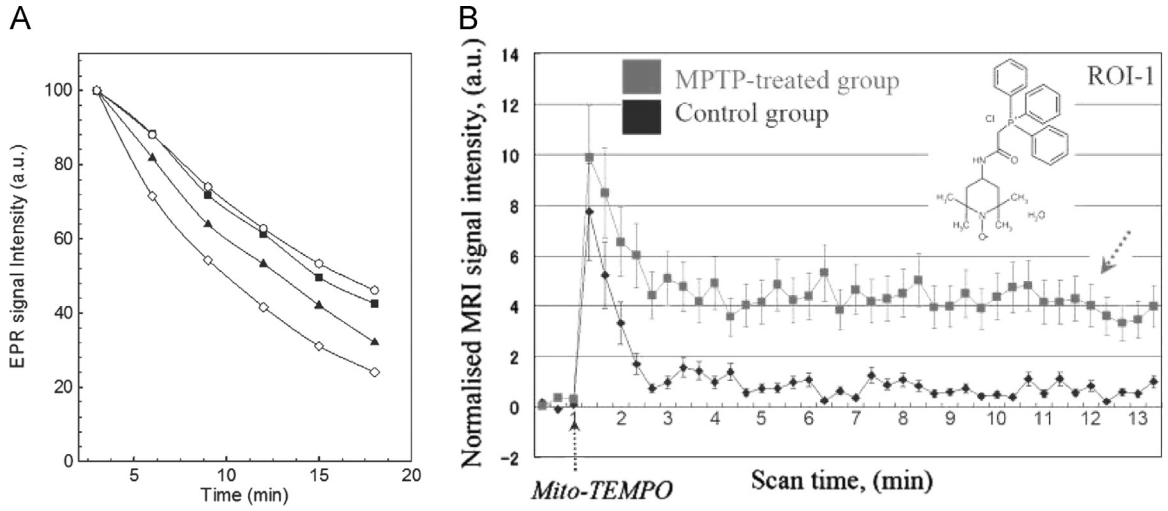

Fig. 8. The decay curves of nitroxides in brains of animals with induced diseases. A. Pharmacokinetics of a nitroxide HM-P (**#10**) in a control mouse and septic mouse head obtained by *in vivo* EPRI [122]. Time course of the *in vivo* EPR signal intensity of HM-P in the control mouse and septic mice injected with LPS. (○) Control mouse head ($t_{1/2}$ =663 s); (◇) mouse injected with LPS only ($t_{1/2}$=374 s); mouse injected with LPS plus aminoguanidine ($t_{1/2}$=535 s) (■); mouse injected with LPS plus allopurinol ($t_{1/2}$ =489 s) (▲). B. Kinetic curves of the nitroxide-enhanced MRI signal in the brain of healthy (bottom line) and MPTP treated mice (top line) [31].

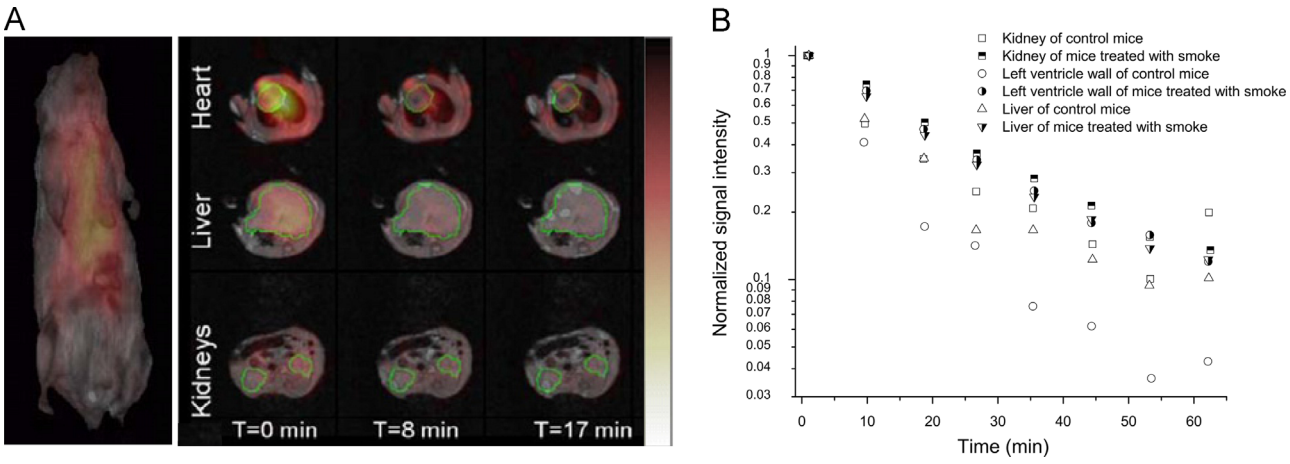

Fig. 9. Images and pharmacokinetics obtained on the hybrid co-imaging instrument, suitable for whole body imaging in both EPR and MR modalities without movement of the animal. A. Whole body MRI image from which transverse sections through selected organs were obtained. Renderings of the superimposed 3D EPRI and 3D proton MRI of mice. The color map is for the EPR intensity (see color bar) of the 3-CP nitroxide probe distribution. Transverse slices through different organs of the animal showing the temporal change of EPR intensity of 3-CP. The green contour depicts the ROI used to calculate the average EPR intensity distribution of the probe. B. Plot of the average signal intensity values over time of the injected 3-CP as measured from the selected ROIs in control and smoke exposed animals. Adapted from [30]. (For interpretation of the references to color in this figure legend,the reader is referred to the web version of this article).

A study on mice with hepatic ischemia-reperfusion injury showed that CV159-Ca^{2+}/calmodulin blockade inhibiting Ca^{2+} overloading has a profound effect on the liver reducing ability [134]. Oxidative stress during ischemia-reperfusion acute renal failure has been studied using EPRI and 3-CP [135]. Decay rates were prolonged 3 days after I/R in both kidneys and liver. In liver they recovered after 7 days, while recovery in kidneys was only partial.

Low molecular weight iron complexes have been detected in iron overload, which occurs in many diseases, and free radical production through oxidative processes is suspected to be the cause of iron toxicity. Free radical reactions have been studied by EPR in an iron overload model [136]. The signal decay of 3-CP detected in liver was significantly enhanced in mice subcutaneously loaded with ferric citrate (Fig. 10) and that enhancement was suppressed by pre-treatment with either desferrioxamine or the chain breaking antioxidant Trolox, but only slightly suppressed by the hydroxyl radical scavenger DMSO.

The redox status in hypertension (HT) has been studied in a mice model by decay of the 3-CP signal in kidneys. Half-lives in HT mice were significantly higher than in control mice. This effect can be reduced by application of the calcium channel blocker azelnidipine and was independent of blood pressure control [137]. Mice that lack the Nrf2 transcription factor develop a lupus-like autoimmune nephritis. Observed half-lives of 3-CP in the upper abdomen in Nrf2 mice, especially in aged ones, were significantly prolonged when compared to young and healthy ones [138]. Mucosal sulfhydryl compounds have been studied in experimental colitis [139]. The decay rates of 3-CP were much slower in colitis and agreed with the time dependent changes in mucosal glutathione. The effect of X-radiation on the reduction of 3-CP in mice liver has been studied to evaluate the potential of EPR in assessing radiation induced oxidative stress [140]. The reduction rate has been accelerated after irradiation, but suppressed by pre-administration of the radioprotector cysteamine.

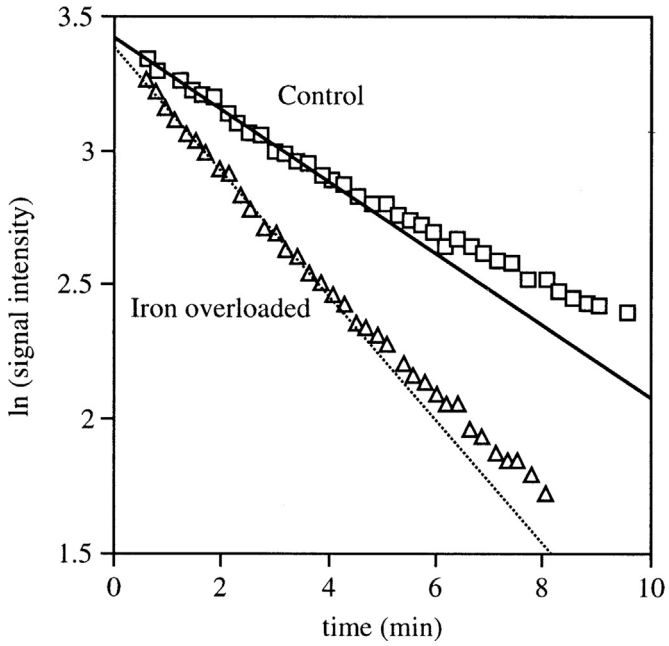

Fig. 10. EPR signal decay of 3-CP in the upper abdomen of mice in an iron overload model. Note a departure of the decay curves from a single-exponential decay [136].

5.4. Tumors

It is well-known that the cancer cells and tissues have different redox abilities from normal tissues. Differences in the redox status between tumors and healthy tissue may originate from hypoxia and increased concentrations of reducing agents in tumors. It is essential to obtain good insight into the redox status of tumors in order to design a proper therapy and estimate the response of tumor to the therapy, since it is well-known that efficiency of radiotherapy depends on oxygenation of tumors. For this purpose reduction of different nitroxides has been studied by *in vivo* EPR (both spectroscopy and imaging) and MRI on animal models. Imaging is a preferable modality due to tumor tissue heterogeneity.

The most studied tumors have been those implanted into the thigh of rodents [28,98,141–144]. A series of studies performed *in vivo* on radiation induced fibrosarcoma (RIF-1) in mice [141–143] generally showed that reduction of all cell-permeable nitroxides (TEMPOL, 3-CP, HM-P) is faster in the tumor bearing leg than in healthy muscle. Fig. 11A illustrates the heterogeneous accumulation of nitroxide in the tumor and heterogeneous distribution of reduction rates. It was also noticed that the amount of nitroxide accumulated in healthy muscle was higher than in the tumor bearing leg at the same time point after injection of the probe. The lower concentrations and faster reduction of nitroxides in the RIF-1 tumor were attributed to the higher concentrations of GSH in the tumor bearing leg. Such a conclusion was supported by the fact that animals treated with the glutathione synthesis inhibitor, buthionine sulphoximine (BSO), led to a substantial decrease in the reduction rate in the tumor (Fig. 11B).

The same authors also investigated the effect of oxygen on the reduction rate of nitroxides. It has been found that the average partial pressure of oxygen (pO_2) in tumors was 3-fold lower than in a normal tissue, which could contribute to the faster reduction of nitroxides in tumors [141]. In tumor bearing mice which were inhaling carbogen, the reduction rate of nitroxide at the tumor site decreased when compared with the air-breathing mice [143]. The significantly decreased heterogeneity of redox maps and narrow distribution of reduction rate constants on frequency plots of carbogen breathing mice indicated that heterogeneity in the redox status could be due to hypoxia and oxygen concentration heterogeneity in a tumor. However, experiments with simultaneous measurements of the pO_2 in tumors and the reduction rate at the region of pO_2 measurements showed rather poor correlation between these parameters, indicating that the extent of oxygenation does not necessarily determine the redox status under air breathing conditions [144].

Studies performed on squamous cell carcinoma (SCCVII), human colon carcinoma and KHT tumors using MRI to monitor the reduction of nitroxides (TEMPOL and 3-CP) also showed faster reduction in all tumor types (different reduction rates for different types) than in normal muscle or other normal tissue [28,98]. Reduction in the muscle was the same in the tumor bearing and contralateral leg [28]. Measurements of the total amount of nitroxide either by MRI *in vivo* or by EPR on tissue homogenates showed that the amount of nitroxides in tumors were similar to those in muscles indicating that different reduction rates are the result of different intracellular bioreduction. This conclusion has been corroborated by the fact that there was no difference in the rate of reduction of membrane impermeable 3-CxP between tumor and muscle [98]. It has been suggested that tissue pO_2 is not the major determinant of the nitroxide reduction *in vivo* [28].

Studies performed on brain tumors (neuroblastoma and glioma) by monitoring the reduction of cell- and BBB-permeable nitrosourea spin probe SLENU (#**8**) and TEMPOL by MRI also

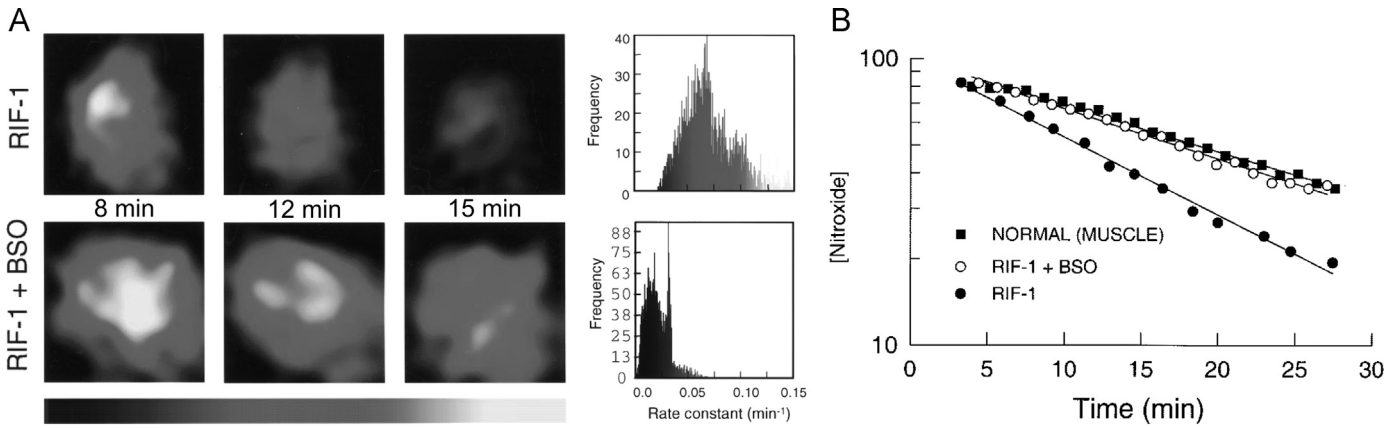

Fig. 11. EPRI of the thigh of a mouse with an implanted RIF-1 tumor. A Selected EPR images of clearance of 3-CP nitroxide in tumors of untreated and BSO treated animals and frequency plot of 3-CP reduction rate constants calculated pixel-by-pixel assuming first-order kinetics. B. The semilog plot showing the whole tissue clearance of nitroxide simultaneously measured in tumors and normal muscle of the contra lateral leg. Images of tumor and muscle used for the measurement of pharmacokinetic data were collected simultaneously in the same animals. Adapted from [142].

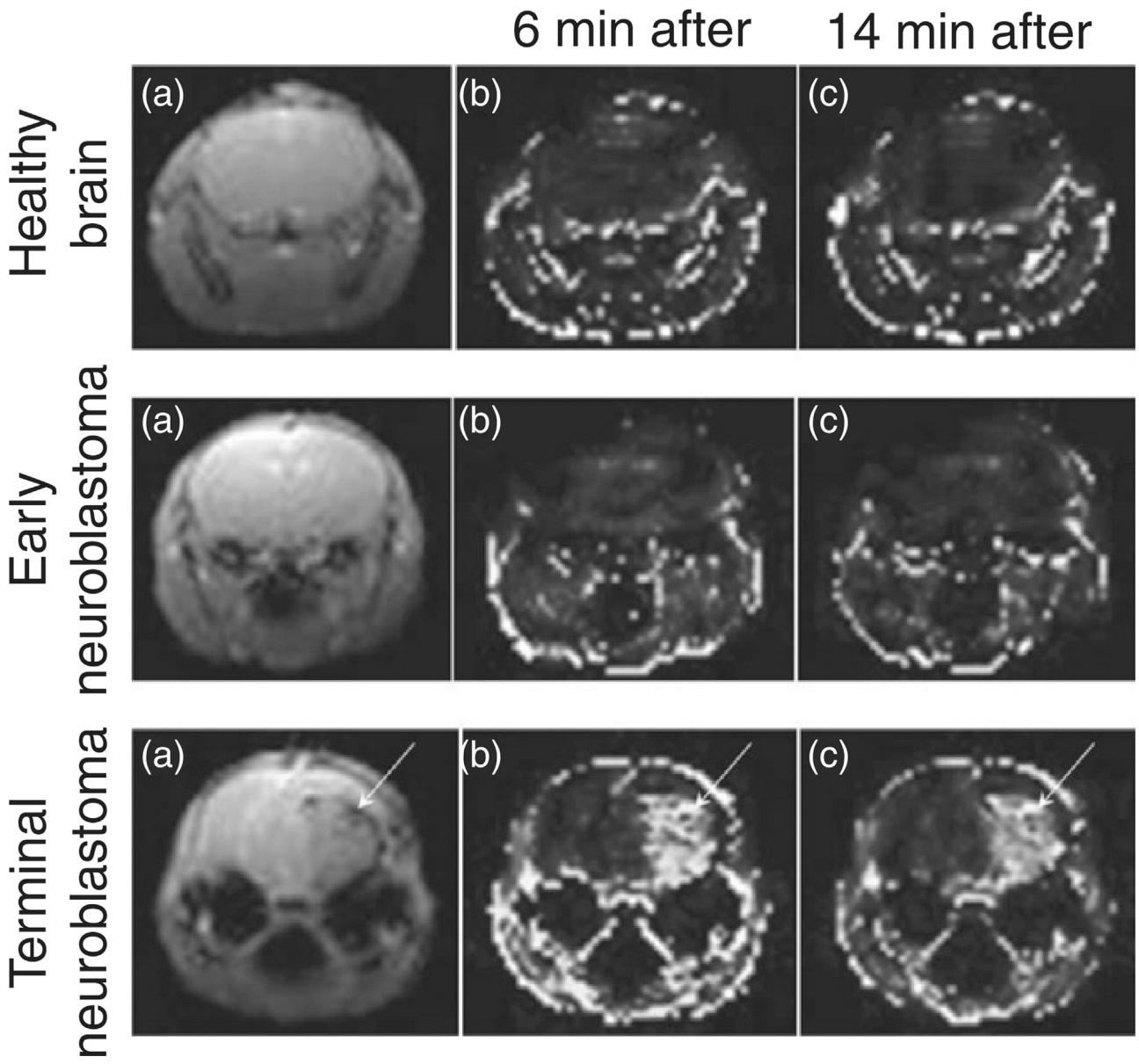

Fig. 12. Nitroxide enhanced MRI images of healthy and tumor bearing mice in the early and terminal stage of disease [146]. Raw MRI images and extracted enhancement images. MRI signal enhancement by nitroxide is clearly seen in the tumor at the terminal stage.

reflected the changed redox status of the tumor when compared to the corresponding tissue of healthy animals [145, 146]. All brain tissues (cancer and non-cancer) in cancer bearing animals were characterized by a long half-life ($t_{1/2} > 14$ min) indicating a high oxidative activity, while brain tissues in healthy mice were characterized by a short half-life ($t_{1/2} < 3$ min) [145]. This study has been complemented by findings that the half-life of nitroxides in the early stages of tumors is comparable to ones in healthy mice, but much shorter than in tumors at terminal stages (Fig. 12). Such behavior has been explained by the highly oxidizing activity of the terminal-stage tumor, whereas an early-stage tumor is characterized by the reducing activity. The explanation was corroborated by profound reoxidation of the injected hydroxylamine form of the probe which occurred only in the terminal stage in tumor bearing mice [146]. An interesting finding was the observation that the redox potential of tissues distant from the primary tumor locus, such as liver and lung, was altered in tumor bearing animals.

An entirely different approach in studying the redox status of the tumor has been performed in a study aimed to measure *in vivo* glutathione in tumors [52]. Authors used the nitroxide probe consisting of two nitroxide rings bound by the S-S bond which due to the pairwise spin exchange of two radical subunits gives an EPR spectrum different from the triplet pattern typical for mononitroxide. Hence, it was possible to follow the reaction between the probe and GSH by recording the increase of the monoradical EPR spectrum from which kinetic parameters and the total amount of GSH can be determined *in vivo*. One of the most important results of this study is that the amount of intracellular GSH in cisplatin resistant tumors is two times higher than in cisplatin sensitive tumors, which is an important contribution towards a better understanding of the mechanisms of action of this widely used antineoplastic agent.

6. Conclusions and look to the future

EPR and MR imaging *in vivo* reached the level of a powerful tool in experimental and preclinical studies of ROS/RNS or the redox

status on animals. As evident from given examples, numerous studies performed previously only on *in vitro* or *ex vivo* samples have been successfully transferred to *in vivo* conditions where basic concepts and hypothesis can be tested under realistic conditions. Here we reviewed only research related to some sort of pathologies but the list of researches related to normal *in vivo* redox biochemistry/physiology is more extensive. The success came from development of more sensitive EPR machines and various EPR/MRI combinations (co-registration, hybrid, OMRI) as well as from development of a host of versatile nitroxide probes. The major problems appear to be the expensiveness of machines and hence their scarcity, as well the lack of coordination between centers where *in vivo* EPR/MRI studies on redox mechanisms are performed.

Consequently, the basic concepts are well understood and directions for future developments are pretty clear. On the instrumental side, further development of hybrid machines, especially OMRI, is an obvious way to go. This approach has been recently extended, albeit in test tubes, to simultaneous imaging of free radical intermediates involved in the mitochondrial electron transport chain and radicals derived from vitamins E and K_1 [147]. This opens a host of possibilities including metabolic imaging in various pathologies and imaging of spin-trapped radicals. The importance of such development lies in the possibility of extending such studies to humans and clinical research. OMRI machines combine almost all MRI capabilities with molecular specificity of EPR which can be useful in diagnosis, but particularly valuable in treatment follow-up studies. Instrumental developments have to be accompanied by developments of specific probes suited for different purposes. Design of new probes with increased stability towards reduction, enhanced sensitivity to oxidative stress, or increased delivery into cells and through the blood–brain barrier is needed and some good research has been recently conducted in that direction [148–151]. Another line of improvement is developing of probes which show specificity towards certain ROS specie or specificity toward certain pathologies such as tumors [152,153]. Due to the scarcity of centers possessing sophisticated equipment, a focused concerted effort on certain cluster of widely relevant pathologies would certainly contribute to the development of the field. For example, studies of neurodegenerative disease (Parkinson, Alzheimer, Amyotrophic Lateral Sclerosis, etc.), for whose development it is almost universally agreed that ROS play a key role, would certainly propel these line of researches towards clinical applications.

Acknowledgment

The authors of this review were supported by the European Cooperation in Science and Technology (COST Action BM1203/EU-ROS). Supported by the Ministry of Education, Science and Technological Development of the Republic of Serbia (Project 41005).

References

[1] G.G. Martinovich, I.V. Martinovich, S.N. Cherenkevich, H. Sauer, Redox buffer capacity of the cell: theoretical and experimental approach, Cell. Biochem. Biophys. 58 (2010) 75–83, http://dx.doi.org/10.1007/s12013-010-9090-3.
[2] Q. Ma, Transcriptional responses to oxidative stress: Pathological and toxicological implications, Pharmacol. Ther. 125 (2010) 376–393, http://dx.doi.org/10.1016/j.pharmthera.2009.11.004.
[3] G. Bartosz, Use of spectroscopic probes for detection of reactive oxygen species, Clin. Chim. Acta 368 (2006) 53–76, http://dx.doi.org/10.1016/j.cca.2005.12.039.
[4] E. Zavoisky, Spin magnetic resonance in the decimeter-wave region, J. Phys. USSR 10 (1946) 197–198.
[5] W. Froncisz, J.S. Hyde, The loop-gap resonator: a new microwave lumped circuit ESR sample structure, J. Magn. Reson. 47 (1982) 515–521, http://dx.doi.org/10.1016/0022-2364(82)90221-9.
[6] A. Sotgiu, Resonator design for *in vivo* ESR spectroscopy, J. Magn. Reson. 65 (1985) 206–214, http://dx.doi.org/10.1016/0022-2364(85)90002-2.
[7] L.J. Berliner, H. Fujii, Magnetic resonance imaging of biological specimens by electron paramagnetic resonance of nitroxide spin labels, Science 227 (1985) 517–519, http://dx.doi.org/10.1126/science.2981437.
[8] L.J. Berliner, H. Fujii, X. Wan, S.J. Lukiewicz, Feasibility study of imaging a living murine tumor by electron paramagnetic resonance, Magn. Reson. Med. 4 (1987) 380–384, http://dx.doi.org/10.1002/mrm.1910040410.
[9] M.M. Maltempo, S.S. Eaton, G.R. Eaton, Spectral-spatial two-dimensional EPR imaging, J. Magn. Reson. 72 (1987) 449–455, http://dx.doi.org/10.1016/0022-2364(87)90149-1.
[10] G. Bačić, F. Demsar, Z. Zolnai, H.M. Swartz, Contrast enhancement in ESR imaging: role of oxygen, Magn. Reson. Med. Biol. 1 (1988) 55–65.
[11] G. Bačić, T. Walczak, F. Demsar, H.M. Swartz, Electron spin resonance imaging of tissues with lipid-rich areas, Magn. Reson. Med. 8 (1988) 209–219, http://dx.doi.org/10.1002/mrm.1910080211.
[12] R.K. Woods, G.G. Bačić, P.C. Lauterbur, H.M. Swartz, Three-dimensional electron spin resonance imaging, J. Magn. Reson. 84 (1989) 247–254, http://dx.doi.org/10.1016/0022-2364(89)90368-5.
[13] J.W. Dobrucki, F. Demsar, T. Walczak, R.K. Woods, G. Bacic, H.M. Swartz, Electron spin resonance microscopy of an *in vitro* tumor model, Br. J. Cancer 61 (1990) 221–224, http://dx.doi.org/10.1038/bjc.1990.41.
[14] G. Bacic, M.J. Nilges, R.L. Magin, T. Walczak, H.M. Swartz, *In vivo* localized ESR spectroscopy reflecting metabolism, Magn. Reson. Med. 10 (1989) 266–272, http://dx.doi.org/10.1002/mrm.1910100211.
[15] H. Utsumi, E. Muto, S. Masuda, A. Hamada, *In vivo* ESR measurement of free radicals in whole mice, Biochem. Biophys. Res. Commun. 172 (1990) 1342–1348, http://dx.doi.org/10.1016/0006-291X(90)91597-L.
[16] M. Ferrari, S. Colacicchi, G. Gualtieri, M.T. Santini, A. Sotgiu, Whole mouse nitroxide free radical pharmacokinetics by low frequency electron paramagnetic resonance, Biochem. Biophys. Res. Commun. 166 (1990) 168–173, http://dx.doi.org/10.1016/0006-291X(90)91926-J.
[17] Y. Miura, H. Utsumi, A. Hamada, Effects of inspired oxygen concentration on *in vivo* redox reaction of nitroxide radicals in whole mice, Biochem. Biophys. Res. Commun. 182 (1992) 1108–1114, http://dx.doi.org/10.1016/0006-291X(92)91846-I.
[18] K. Takeshita, H. Utsumi, A. Hamada, ESR measurement of radical clearance in lung of whole mouse, Biochem. Biophys. Res. Commun. 177 (1991) 874–880, http://dx.doi.org/10.1016/0006-291X(91)91871-9.
[19] S. Ishida, S. Matsumoto, H. Yokoyama, N. Mori, H. Kumashiro, N. Tsuchihashi, T. Ogata, M. Yamada, M. Ono, T. Kitajima, H. Kamada, E. Yoshida, An ESR-CT imaging of the head of a living rat receiving an administration of a nitroxide radical, Magn. Reson. Imaging 10 (1992) 109–114, http://dx.doi.org/10.1016/0730-725X(92)90379-E.
[20] F. Gomi, H. Utsumi, A. Hamada, M. Matsuo, Aging retards spin clearance from mouse brain and food restriction prevents its age-dependent retardation, Life Sci. 52 (1993) 2027–2033, http://dx.doi.org/10.1016/0024-3205(93)90687-X.
[21] M. Alecci, M. Ferrari, V. Quaresima, A. Sotgiu, C.L. Ursini, Simultaneous 280 MHz EPR imaging of rat organs during nitroxide free radical clearance, Biophys. J. 67 (1994) 1274–1279, http://dx.doi.org/10.1016/S0006-3495(94)80599-5.
[22] A.M. Komarov, J. Joseph, C.-S. Lai, In vivo pharmacokinetics of nitroxides in mice, Biochem. Biophys. Res. Commun. 201 (1994) 1035–1042, http://dx.doi.org/10.1006/bbrc.1994.1806.
[23] L.J. Berliner (Ed.), In Vivo EPR (ESR): Theory and Application, Biological Magnetic Resonance, Vol. 18, Kluwer Academic/Plenum, New York, http://dx.doi.org/10.1007/978-1-4615-0061-2.
[24] H.M. Swartz, M. Sentjurc, P.D. Morse, Cellular metabolism of water-soluble nitroxides: effect on rate of reduction of cell/nitroxide ratio, oxygen concentrations and permeability of nitroxides, Biochim. Biophys. Acta 888 (1986) 82–90, http://dx.doi.org/10.1016/0167-4889(86)90073-X.
[25] H.M. Swartz, Use of nitroxides to measure redox metabolism in cells and tissues, J. Chem. Soc. Faraday Trans. 1: Phys. Chem. Condens. Ph. 83 (1987) 191–202, http://dx.doi.org/10.1039/F19878300191.
[26] R.C. Brasch, Work in progress: methods of contrast enhancement for NMR imaging and potential applications. A subject review, Radiology 147 (1983) 781–788, http://dx.doi.org/10.1148/radiology.147.3.6342034.
[27] F. Hyodo, K.-H. Chuang, A.G. Goloshevsky, A. Sulima, G.L. Griffiths, J. B. Mitchell, A.P. Koretsky, M.C. Krishna, Brain redox imaging using blood-brain barrier-permeable nitroxide MRI contrast agent, J. Cereb. Blood Flow Metab. 28 (2008) 1165–1174, http://dx.doi.org/10.1038/jcbfm.2008.5.
[28] R.M. Davis, S. Matsumoto, M. Bernardo, A. Sowers, K.-I. Matsumoto, M. C. Krishna, J.B. Mitchell, Magnetic resonance imaging of organic contrast agents in mice: capturing the whole-body redox landscape, Free Radic. Biol. Med. 50 (2011) 459–468, http://dx.doi.org/10.1016/j.freeradbiomed.2010.11.028.
[29] R.M. Davis, A.L. Sowers, W. DeGraff, M. Bernardo, A. Thetford, M.C. Krishna, J. B. Mitchell, A novel nitroxide is an effective brain redox imaging contrast agent and *in vivo* radioprotector, Free Radic. Biol. Med. 51 (2011) 780–790, http://dx.doi.org/10.1016/j.freeradbiomed.2011.05.019.
[30] G.L. Caia, O.V. Efimova, M. Velayutham, M.A. El-Mahdy, T.M. Abdelghany, E. Kesselring, S. Petryakov, Z. Sun, A. Samouilov, J.L. Zweier, Organ specific mapping of *in vivo* redox state in control and cigarette smoke-exposed mice using EPR/NMR co-imaging, J. Magn. Reson. 216 (2012) 21–27, http://dx.doi.

org/10.1016/j.jmr.2011.10.017.
[31] Z. Zhelev, R. Bakalova, I. Aoki, D. Lazarova, T. Saga, Imaging of superoxide generation in the dopaminergic area of the brain in Parkinson's disease, using mito-TEMPO, ACS Chem. Neurosci. 4 (2013) 1439–1445, http://dx.doi.org/10.1021/cn400159h.
[32] M. Elas, K. Ichikawa, H.J. Halpern, Oxidative stress imaging in live animals with techniques based on electron paramagnetic resonance, Radiat. Res. 177 (2012) 514–523, http://dx.doi.org/10.1667/RR2668.1.
[33] H.M. Swartz, The measurement of oxygen in vivo using EPR techniques. In vivo EPR (ESR): theory and application, in: L.J. Berliner (Ed.), Biological Magnetic Resonance, Vol. 18, Kluwer Academic/Plenum, New York, 2003, pp. 403–440, http://dx.doi.org/10.1007/978-1-4615-0061-2_15.
[34] R. Ahmad, P. Kuppusamy, Theory, instrumentation, and applications of electron paramagnetic resonance oximetry, Chem. Rev. 110 (2010) 3212–3236, http://dx.doi.org/10.1021/cr900396q.
[35] S. Subramanian, N. Devasahayam, A. McMillan, S. Matsumoto, J. P. Munasinghe, K. Saito, J.B. Mitchell, G.V.R. Chandramouli, M.C. Krishna, Reporting of quantitative oxygen mapping in EPR imaging, J. Magn. Reson. 214 (2012) 244–251, http://dx.doi.org/10.1016/j.jmr.2011.11.013.
[36] G. He, Y. Deng, H. Li, P. Kuppusamy, J.L. Zweier, EPR/NMR co-imaging for anatomic registration of free-radical images, Magn. Reson. Med. 47 (2002) 571–578, http://dx.doi.org/10.1002/mrm.10077.
[37] F. Hyodo, K. Yasukawa, K.-I. Yamada, H. Utsumi, Spatially resolved time-course studies of free radical reactions with an EPRI/MRI fusion technique, Magn. Reson. Med. 56 (2006) 938–943, http://dx.doi.org/10.1002/mrm.21019.
[38] H. Fujii, M. Aoki, T. Haishi, K. Itoh, M. Sakata, Development of an ESR/MR dual-imaging system as a tool to detect bioradicals, Magn. Reson. Med. Sci. 5 (2006) 17–23, http://dx.doi.org/10.2463/mrms.5.17.
[39] A. Samouilov, G.L. Caia, E. Kesselring, S. Petryakov, T. Wasowicz, J.L. Zweier, Development of a hybrid EPR/NMR coimaging system, Magn. Reson. Med. 58 (2007) 156–166, http://dx.doi.org/10.1002/mrm.21205.
[40] D.J. Lurie, D.M. Bussell, L.H. Bell, J.R. Mallard, Proton–electron double magnetic resonance imaging of free radical solutions, J. Magn. Reson. 76 (1988) 366–370, http://dx.doi.org/10.1016/0022-2364(88)90123-0.
[41] M.C. Krishna, S. English, K. Yamada, J. Yoo, R. Murugesan, N. Devasahayam, J. A. Cook, K. Golman, J.H. Ardenkjaer-Larsen, S. Subramanian, J.B. Mitchell, Overhauser enhanced magnetic resonance imaging for tumor oximetry: Coregistration of tumor anatomy and tissue oxygen concentration, Proc. Natl. Acad. Sci. USA 99 (2002) 2216–2221, http://dx.doi.org/10.1073/pnas.042671399.
[42] M. Yamato, T. Shiba, K.-I. Yamada, T. Watanabe, H. Utsumi, Noninvasive assessment of the brain redox status after transient middle cerebral artery occlusion using Overhauser-enhanced magnetic resonance imaging, J. Cereb. Blood Flow Metab. 29 (2009) 1655–1664, http://dx.doi.org/10.1038/jcbfm.2009.84.
[43] M. Yamato, T. Shiba, T. Naganuma, K. Ichikawa, H. Utsumi, K.-I. Yamada, Overhauser-enhanced magnetic resonance imaging characterization of mitochondria functional changes in the 6-hydroxydopamine rat model, Neurochem. Int. 59 (2011) 804–811, http://dx.doi.org/10.1016/j.neuint.2011.08.010.
[44] D.J. Lurie, M.A. Foster, D. Yeung, J.M.S. Hutchison, Design, construction and use of a large-sample field-cycled PEDRI imager, Phys. Med. Biol. 43 (1998) 1877–1886, http://dx.doi.org/10.1088/0031-9155/43/7/008.
[45] K.-I. Matsumoto, S. Subramanian, R. Murugesan, J.B. Mitchell, M.C. Krishna, Spatially resolved biologic information from *in vivo* EPRI, OMRI, and MRI, Antioxid. Redox Signal. 9 (2007) 1125–1141, http://dx.doi.org/10.1089/ars.2007.1638.
[46] F. Hyodo, R. Murugesan, K.-I. Matsumoto, E. Hyodo, S. Subramanian, J. B. Mitchell, M.C. Krishna, Monitoring redox-sensitive paramagnetic contrast agent by EPRI, OMRI and MRI, J. Magn. Reson. 190 (2008) 105–112, http://dx.doi.org/10.1016/j.jmr.2007.10.013.
[47] S. Colacicchi, M. Ferrari, A. Sotgiu, *In vivo* electron paramagnetic resonance spectroscopy/imaging: first experiences, problems, and perspectives, Int. J. Biochem. 24 (1992) 205–214, http://dx.doi.org/10.1016/0020-711X(92)90248-Y.
[48] G.S. Timmins, K.J. Liu, E.J.H. Bechara, Y. Kotake, H.M. Swartz, Trapping of free radicals with direct in vivo EPR detection: a comparison of 5,5-dimethyl-1-pyrroline-*N*-oxide and 5-diethoxyphosphoryl-5-methyl-1-pyrroline-*N*-oxide as spin traps for $HO^{\bullet}$ and $SO_4^{\bullet-}$, Free Radic. Biol. Med. 27 (1999) 329–333, http://dx.doi.org/10.1016/S0891-5849(99)00049-0.
[49] N. Khan, H. Swartz, Measurements *in vivo* of parameters pertinent to ROS/RNS using EPR spectroscopy, Mol. Cell. Biochem. 234/235 (2002) 341–357, http://dx.doi.org/10.1023/A:1015938528432.
[50] F. Hyodo, S. Matsumoto, N. Devasahayam, C. Dharmaraj, S. Subramanian, J. B. Mitchell, M.C. Krishna, Pulsed EPR imaging of nitroxides in mice, J. Magn. Reson. 197 (2009) 181–185, http://dx.doi.org/10.1016/j.jmr.2008.12.018.
[51] H. Fujii, H. Sato-Akaba, K. Kawanishi, H. Hirata, Mapping of redox status in a brain-disease mouse model by three-dimensional EPR imaging, Magn. Reson. Med. 65 (2011) 295–303, http://dx.doi.org/10.1002/mrm.22598.
[52] G.I. Roshchupkina, A.A. Bobko, A. Bratasz, V.A. Reznikov, P. Kuppusamy, V. V. Khramtsov, *In vivo* EPR measurement of glutathione in tumor-bearing mice using improved disulfide biradical probe, Free Radic. Biol. Med. 45 (2008) 312–320, http://dx.doi.org/10.1016/j.freeradbiomed.2008.04.019.
[53] G. He, V.K. Kutala, P. Kuppusamy, J.L. Zweier, In vivo measurement and mapping of skin redox stress induced by ultraviolet light exposure, Free Radic. Biol. Med. 36 (2004) 665–672, http://dx.doi.org/10.1016/j.freeradbiomed.2003.11.024.
[54] A.T. Yordanov, K.-I. Yamada, M.C. Krishna, A. Russo, J. Yoo, S. English, J. B. Mitchell, M.W. Brechbiel, Acyl-protected hydroxylamines as spin label generators for EPR brain imaging, J. Med. Chem. 45 (2002) 2283–2288, http://dx.doi.org/10.1021/jm0105169.
[55] G.J. Giotta, H.H. Wang, Reduction of nitroxide free radicals by biological materials, Biochem. Biophys. Res. Commun. 46 (1972) 1576–1580, http://dx.doi.org/10.1016/0006-291X(72)90788-7.
[56] K. Chen, H.M. Swartz, The products of the reduction of doxyl stearates in cells are hydroxylamines as shown by oxidation by ^{15}N-perdeuterated Tempone, Biochim. Biophys. Acta 992 (1989) 131–133, http://dx.doi.org/10.1016/0304-4165(89)90060-3.
[57] H.M. Swartz, Principles of the metabolism of nitroxides and their implications for spin trapping, Free Radic. Res. Commun. 9 (1990) 399–405, http://dx.doi.org/10.3109/10715769009145700.
[58] W.R. Couet, R.C. Brasch, G. Sosnovsky, J. Lukszo, I. Prakash, C.T. Gnewech, T. N. Tozer, Influence of chemical structure of nitroxyl spin labels on their reduction by ascorbic acid, Tetrahedron 41 (1985) 1165–1172, http://dx.doi.org/10.1016/S0040-4020(01)96516-0.
[59] J.F.W. Keana, S. Pou, G.M. Rosen, Nitroxides as potential contrast enhancing agents for MRI application: influence of structure on the rate of reduction by rat hepatocytes, whole liver homogenate, subcellular fractions, and ascorbate, Magn. Reson. Med. 5 (1987) 525–536, http://dx.doi.org/10.1002/mrm.1910050603.
[60] S. Morris, G. Sosnovsky, B. Hui, C.O. Huber, N.U.M. Rao, H.M. Swartz, Chemical and electrochemical reduction rates of cyclic nitroxides (nitroxyls), J. Pharm. Sci. 80 (1991) 149–152, http://dx.doi.org/10.1002/jps.2600800212.
[61] A. Iannone, H. Hu, A. Tomasi, V. Vannini, H.M. Swartz, Metabolism of aqueous soluble nitroxides in hepatocytes: effects of cell integrity, oxygen, and structure of nitroxides, Biochim. Biophys. Acta 991 (1989) 90–96, http://dx.doi.org/10.1016/0304-4165(89)90033-0.
[62] K. Chen, J.F. Glockner, P.D. Morse, H.M. Swartz, Effects of oxygen on the metabolism of nitroxide spin labels in cells, Biochemistry 28 (1989) 2496–2501, http://dx.doi.org/10.1021/bi00432a022.
[63] A. Ueda, S. Nagase, H. Yokoyama, M. Tada, H. Noda, H. Ohya, H. Kamada, A. Hirayama, A. Koyama, Importance of renal mitochondria in the reduction of TEMPOL, a nitroxide radical, Mol. Cell. Biochem. 244 (2003) 119–124, http://dx.doi.org/10.1023/A:1022477530291.
[64] A. Iannone, A. Tomasi, V. Vannini, H.M. Swartz, Metabolism of nitroxide spin labels in subcellular fraction of rat liver: I. Reduction by microsomes, Biochim. Biophys. Acta 1034 (1990) 285–289, http://dx.doi.org/10.1016/0304-4165(90)90052-X.
[65] Y. Samuni, J. Gamson, A. Samuni, K. Yamada, A. Russo, M.C. Krishna, J. B. Mitchell, Factors influencing nitroxide reduction and cytotoxicity in vitro, Antioxid. Redox Signal. 6 (2004) 587–595, http://dx.doi.org/10.1089/152308604773934341.
[66] A. Iannone, A. Tomasi, V. Vannini, H.M. Swartz, Metabolism of nitroxide spin labels in subcellular fractions of rat-liver. II. Reduction in the cytosol, Biochim. Biophys. Acta 1034 (1990) 290–293, http://dx.doi.org/10.1016/0304-4165(90)90053-Y.
[67] K.-Y. Chen, M.G. McLaughlin, Differences in the reduction kinetics of incorporated spin labels in undifferentiated and differentiated mouse neuroblastoma cells, Biochim. Biophys. Acta 845 (1985) 189–195, http://dx.doi.org/10.1016/0167-4889(85)90176-4.
[68] T. Suzuki-Nishimura, H.M. Swartz, Reduction of lipid-soluble nitroxides in CHO cells and macrophage tumor cells, Free Radic. Biol. Med. 17 (1994) 473–479, http://dx.doi.org/10.1016/0891-5849(94)90174-0.
[69] T. Suzuki-Nishimura, H.M. Swartz, Characterization of redox activity in resting and activated mast cells by reduction and reoxidation of lipophilic nitroxides, Gen. Pharmacol. 31 (1998) 617–623, http://dx.doi.org/10.1016/S0306-3623(98)00066-4.
[70] K. Chen, H.M. Swartz, Oxidation of hydroxylamines to nitroxide spin labels in living cells, Biochim. Biophys. Acta 970 (1988) 270–277, http://dx.doi.org/10.1016/0167-4889(88)90126-7.
[71] T. Yamaguchi, T. Nakano, E. Kimoto, Oxidation of nitroxide radicals by the reaction of hemoglobin with hydrogen peroxide, Biochem. Biophys. Res. Commun. 120 (1984) 534–539, http://dx.doi.org/10.1016/0006-291X(84)91287-7.
[72] M.C. Krishna, A. Samuni, J. Taira, S. Goldstein, J.B. Mitchell, A. Russo, Stimulation by nitroxides of catalase-like activity of hemeproteins – kinetics and mechanism, J. Biol. Chem. 271 (1996) 26018–26025, http://dx.doi.org/10.1074/jbc.271.42.26018.
[73] M.C. Krishna, D.A. Grahame, A. Samuni, J.B. Mitchell, A. Russo, Oxoammonium cation intermediate in the nitroxide-catalyzed dismutation of superoxide, Proc. Natl. Acad. Sci. USA 89 (1992) 5537–5541, http://dx.doi.org/10.1073/pnas.89.12.5537.
[74] S. Goldstein, G. Merenyi, A. Russo, A. Samuni, The role of oxoammonium cation in the SOD-mimic activity of cyclic nitroxides, J. Am. Chem. Soc. 125 (2003) 789–795, http://dx.doi.org/10.1021/ja028190w.
[75] S. Goldstein, A. Samuni, K. Hideg, G. Merenyi, Structure-activity relationship of cyclic nitroxides as SOD mimics and scavengers of nitrogen dioxide and carbonate radicals, J. Phys. Chem. A 110 (2006) 3679–3685, http://dx.doi.org/10.1021/jp056869r.
[76] S. Goldstein, A. Samuni, A. Russo, Reaction of cyclic nitroxides with nitrogen dioxide: the intermediacy of the oxoammonium cations, J. Am. Chem. Soc.

125 (2003) 8364–8370, http://dx.doi.org/10.1021/ja035286x.
[77] S. Goldstein, A. Samuni, G. Merenyi, Reactions of nitric oxide, peroxynitrite, and carbonate radicals with nitroxides and their corresponding oxoammonium cations, Chem. Res. Toxicol. 17 (2004) 250–257, http://dx.doi.org/10.1021/tx0342363.
[78] A. Samuni, S. Goldstein, A. Russo, J.B. Mitchell, M.C. Krishna, P. Neta, Kinetics and mechanism of hydroxyl radical and OH-adduct radical reactions with nitroxides and with their hydroxylamines, J. Am. Chem. Soc. 124 (2002) 8719–8724, http://dx.doi.org/10.1021/ja017587h.
[79] O.M. Lardinois, D.A. Maltby, K.F. Medzihradszky, P.R.O. de Montellano, K. B. Tomer, R.P. Mason, L.J. Deterding, Spin scavenging analysis of myoglobin protein-centered radicals using stable nitroxide radicals: characterization of oxoammonium cation-induced modifications, Chem. Res. Toxicol. 22 (2009) 1034–1049, http://dx.doi.org/10.1021/tx9000094.
[80] S. Goldstein, A. Samuni, Kinetics and mechanism of peroxyl radical reactions with nitroxides, J. Phys. Chem. A 111 (2007) 1066–1072, http://dx.doi.org/10.1021/jp0655975.
[81] A. Israeli, M. Patt, M. Oron, A. Samuni, R. Kohen, S. Goldstein, Kinetics and mechanism of the comproportionation reaction between oxoammonium cation and hydroxylamine derived from cyclic nitroxides, Free Radic. Biol. Med. 38 (2005) 317–324, http://dx.doi.org/10.1016/j.freeradbiomed.2004.09.037.
[82] I. Dragutan, R.J. Mehlhorn, Modulation of oxidative damage by nitroxide free radicals, Free Radic. Res. 41 (2007) 303–315, http://dx.doi.org/10.1080/10715760601089356.
[83] P. Bar-On, M. Mohsen, R. Zhang, E. Feigin, M. Chevion, A. Samuni, Kinetics of nitroxide reaction with iron(II), J. Am. Chem. Soc. 121 (1999) 8070–8073, http://dx.doi.org/10.1021/ja990623g.
[84] R. Zhang, S. Goldstein, A. Samuni, Kinetics of superoxide-induced exchange among nitroxide antioxidants and their oxidized and reduced forms, Free Radic. Biol. Med. 26 (1999) 1245–1252, http://dx.doi.org/10.1016/S0891-5849(98)00328-1.
[85] M. Mojović, A. Popović-Bijelić, A. Pavićević, S. Stamenković, M. Jovanović, P. R. Andjus, G. Bačić. Probing spin-probes. The EPR in vivo study of pharmacokinetics of two spin-probes, in: Proceedings of the 12th International Conference on Fundamental and Applied Aspects of Physical Chemistry, Belgrade, Serbia, 2014, pp. 550–553.
[86] N. Nishino, H. Yasui, H. Sakurai, In vivo L-band ESR and quantitative pharmacokinetic analysis of stable spin probes in rats and mice, Free. Radic. Res. 31 (1999) 35–51, http://dx.doi.org/10.1080/10715769900300581.
[87] T. Sano, F. Umeda, T. Hashimoto, H. Nawata, H. Utsumi, Oxidative stress measurement by in vivo electron spin resonance spectroscopy in rats with streptozotocin-induced diabetes, Diabetologia 41 (1998) 1355–1360, http://dx.doi.org/10.1007/s001250051076.
[88] V. Quaresima, M. Alecci, M. Ferrari, A. Sotgiu, Whole rat electron paramagnetic resonance imaging of a nitroxide free radical by a radio frequency (280 MHz) spectrometer, Biochem. Biophys. Res. Commun. 183 (1992) 829–835, http://dx.doi.org/10.1016/0006-291X(92)90558-3.
[89] H. Sano, K.-I. Matsumoto, H. Utsumi, Synthesis and imaging of blood-brain-barrier permeable nitroxyl-probes for free radical reactions in brain of living mice, Biochem. Mol. Biol. Int. 42 (1997) 641–647, http://dx.doi.org/10.1080/15216549700203051.
[90] H. Sano, M. Naruse, K.-I. Matsumoto, T. Oi, H. Utsumi, A new nitroxyl-probe with high retention in the brain and its application for brain imaging, Free Radic. Biol. Med. 28 (2000) 959–969, http://dx.doi.org/10.1016/S0891-5849(00)00184-2.
[91] H. Utsumi, H. Sano, M. Naruse, K.-I. Matsumoto, K. Ichikawa, T. Oi, Nitroxyl probes for brain research and their application to brain imaging, Methods Enzym. 352 (2002) 494–506, http://dx.doi.org/10.1016/S0076-6879(02)52043-7.
[92] H. Yokayama, O. Itoh, M. Aoyama, H. Obara, H. Ohya, H. Kamada, *In vivo* temporal EPR imaging of the brain of rats by using two types of blood-brain barrier-permeable nitroxide radicals, Magn. Reson. Imaging 20 (2002) 277–284, http://dx.doi.org/10.1016/S0730-725X(02)00491-5.
[93] B. Gallez, G. Bacic, F. Goda, J. Jiang, J.A. O'Hara, J.F. Dunn, H.M. Swartz, Use of nitroxides for assessing perfusion, oxygenation, and viability of tissues: *in vivo* EPR and MRI studies, Magn. Reson. Med. 35 (1996) 97–106, http://dx.doi.org/10.1002/mrm.1910350113.
[94] S.M. Hahn, M.C. Krishna, A.M. DeLuca, D. Coffin, J.B. Mitchell, Evaluation of the hydroxylamine Tempol-H as an in vivo radioprotector, Free Radic. Biol. Med. 28 (2000) 953–958, http://dx.doi.org/10.1016/S0891-5849(00)00176-3.
[95] M. Yamato, T. Egashira, H. Utsumi, Application of in vivo ESR spectroscopy to measurement of cerebrovascular ROS generation in stroke, Free Radic. Biol. Med. 35 (2003) 1619–1631, http://dx.doi.org/10.1016/j.freeradbiomed.2003.09.013.
[96] Z. Zhelev, K.-I. Matsumoto, V. Gadjeva, R. Bakalova, I. Aoki, A. Zheleva, K. Anzai, EPR signal reduction kinetic of several nitroxyl derivatives in blood *in vitro* and *in vivo*, Gen. Physiol. Biophys. 28 (2009) 356–362, http://dx.doi.org/10.4149/gpb_2009_04_356.
[97] K.-I. Matsumoto, M.C. Krishna, J.B. Mitchell, Novel pharmacokinetic measurement using electron paramagnetic resonance spectroscopy and simulation of in vivo decay of various nitroxyl spin probes in mouse blood, J. Pharmacol. Exp. Ther. 310 (2004) 1076–1083, http://dx.doi.org/10.1124/jpet.104.066647.
[98] F. Hyodo, K.-I. Matsumoto, A. Matsumoto, J.B. Mitchell, M.C. Krishna, Probing the intracellular redox status of tumors with magnetic resonance imaging and redox-selective contrast agent, Cancer Res. 66 (2006) 9921–9928, http://dx.doi.org/10.1158/0008-5472.CAN-06-0879.
[99] Z. Zhelev, R. Bakalova, I. Aoki, K.-I. Matsumoto, V. Gadjeva, K. Anzai, I. Kanno, Nitroxyl radicals for labeling of conventional therapeutics and noninvasive magnetic resonance imaging of their permeability for blood-brain barrier: relationship between structure, blood clearance, and MRI signal dynamics in the brain, Mol. Pharm. 6 (2009) 504–512, http://dx.doi.org/10.1021/mp800175k.
[100] H.J. Halpern, M. Peric, C. Yu, E.D. Barth, G.V.R. Chandramouli, In vivo spin-label murine pharmacodynamics using low-frequency electron paramagnetic resonance imaging, Biophys. J. 71 (1996) 403–409, http://dx.doi.org/10.1016/S0006-3495(96)79241-X.
[101] K. Saito, K. Takeshita, K. Anzai, T. Ozawa, Pharmacokinetic study of acyl-protected hydroxylamine probe, 1-acetoxy-3-carbamoyl-2,2,5,5-tetramethylpyrrolidine, for in vivo measurements of reactive oxygen species, Free Radic. Biol. Med. 36 (2004) 517–525, http://dx.doi.org/10.1016/j.freeradbiomed.2003.11.010.
[102] K. Mäder, G. Bacic, H.M. Swartz, *In vivo* detection of anthralin-derived free radicals in the skin of hairless mice by low-frequency electron paramagnetic resonance spectroscopy, J. Investig. Dermatol. 104 (1995) 514–517, http://dx.doi.org/10.1111/1523-1747.ep12605998.
[103] E. Vanea, N. Charlier, J. DeWever, M. Dinguizli, O. Feron, J.-F. Baurain, B. Gallez, Molecular electron paramagnetic resonance imaging of melanin in melanomas: a proof-of-concept, NMR Biomed. 21 (2008) 296–300, http://dx.doi.org/10.1002/nbm.1241.
[104] N. Khan, B.B. Williams, H.M. Swartz, Clinical applications of in vivo EPR: rationale and initial results, Appl. Magn. Reson. 30 (2006) 185–199, http://dx.doi.org/10.1007/BF03166718.
[105] J. Fuchs, N. Groth, T. Herrling, R. Milbradt, G. Zimmer, L. Packer, Electron paramagnetic resonance (EPR) imaging in skin: biophysical and biochemical microscopy, J. Investig. Dermatol. 98 (1992) 713–719, http://dx.doi.org/10.1111/1523-1747.ep12499919.
[106] J. Fuchs, H.J. Freisleben, M. Podda, G. Zimmer, R. Milbradt, L. Packer, Nitroxide radical biostability in skin, Free. Radic. Biol. Med. 15 (1993) 415–423, http://dx.doi.org/10.1016/0891-5849(93)90041-R.
[107] J. Fuchs, N. Groth, T. Herrling, Cutaneous tolerance to nitroxide free radicals in human skin, Free Radic. Biol. Med. 24 (1998) 643–648, http://dx.doi.org/10.1016/S0891-5849(97)00322-5.
[108] V. Gabrijelčič, M. Šentjurc, M. Schara, The measurement of liposome entrapped molecules' penetration into the skin: a 1D-EPR and EPR kinetic imaging study, Int. J. Pharm. 102 (1994) 151–158, http://dx.doi.org/10.1016/0378-5173(94)90050-7.
[109] M. Šentjurc, K. Vrhovnik, J. Kristl, Liposomes as a topical delivery system: the role of size on transport studied by EPR imaging method, J. Control. Release 59 (1999) 87–97, http://dx.doi.org/10.1016/S0168-3659(98)00181-3.
[110] J. Fuchs, N. Groth, T. Herrling, G. Zimmer, Electron paramagnetic resonance studies on nitroxide radical 2,2,5,5-tetramethyl-4-piperidin-1-oxyl (TEMPO) redox reactions in human skin, Free Radic. Biol. Med. 22 (1997) 967–976, http://dx.doi.org/10.1016/S0891-5849(96)00433-9.
[111] T. Herrling, K. Jung, J. Fuchs, Measurements of UV-generated free radicals/reactive oxygen species (ROS) in skin, Spectrochim. Acta Part A 63 (2006) 840–845, http://dx.doi.org/10.1016/j.saa.2005.10.013.
[112] K. Takeshita, C. Chi, H. Hirata, M. Ono, T. Ozawa, In vivo generation of free radicals in the skin of live mice under ultraviolet light, measured by L-band EPR spectroscopy, Free Radic. Biol. Med. 40 (2006) 876–885, http://dx.doi.org/10.1016/j.freeradbiomed.2005.10.049.
[113] T. Herrling, J. Fuchs, J. Rehberg, N. Groth, UV-induced free radicals in the skin detected by ESR spectroscopy and imaging using nitroxides, Free. Radic. Biol. Med. 35 (2003) 59–67, http://dx.doi.org/10.1016/S0891-5849(03)00241-7.
[114] K. Takeshita, T. Takajo, H. Hirata, M. Ono, H. Utsumi, *In vivo* oxygen radical generation in the skin of the protoporphyria model mouse with visible light exposure: an L-band ESR study, J. Investig. Dermatol. 122 (2004) 1463–1470, http://dx.doi.org/10.1111/j.0022-202X.2004.22601.x.
[115] G. He, A. Samouilov, P. Kuppusamy, J.L. Zweier, *In vivo* EPR imaging of the distribution and metabolism of nitroxide radicals in human skin, J. Magn. Reson. 148 (2001) 155–164, http://dx.doi.org/10.1006/jmre.2000.2226.
[116] B.A. Jurkiewicz, G.R. Buettner, Ultraviolet light-induced free radical formation in skin: an electron paramagnetic resonance study, Photochem. Photobiol. 59 (1994) 1–4, http://dx.doi.org/10.1111/j.1751-1097.1994.tb04993.x.
[117] B.A. Jurkiewicz, G.R. Buettner, EPR detection of free radicals in UV-irradiated skin: mouse *versus* human, Photochem. Photobiol. 64 (1996) 918–922, http://dx.doi.org/10.1111/j.1751-1097.1996.tb01856.x.
[118] H. Yokoyama, S. Morinobu, Y. Ueda, EPRI to estimate the in vivo intracerebral reducing ability in adolescent rats subjected to neonatal isolation, J. Magn. Reson. Imaging 23 (2006) 637–640, http://dx.doi.org/10.1002/jmri.20560.
[119] H. Yokoyama, Y. Ueda, O. Itoh, T. Ikeda, J.I. Noor, T. Ikenoue, EPR imaging to estimate the in vivo intracerebral reducing ability of mature rats after neonatal hypoxic–ischemic brain injury, Magn. Reson. Imaging 22 (2004) 1305–1309, http://dx.doi.org/10.1016/j.mri.2004.09.003.
[120] H. Yokoyama, Y. Lin, O. Itoh, Y. Ueda, A. Nakajima, T. Ogata, T. Sato, H. Ohya-Nishiguchi, H. Kamada, EPR imaging for in vivo analysis of the half-life of a nitroxide radical in the hippocampus and cerebral cortex of rats after epileptic seizures, Free Radic. Biol. Med. 27 (1999) 442–448, http://dx.doi.org/10.1016/S0891-5849(99)00093-3.
[121] H. Yokoyama, O. Itoh, M. Aoyama, H. Obara, H. Ohya, H. Kamada, In vivo EPR imaging by using an acyl-protected hydroxylamine to analyze intracerebral

oxidative stress in rats after epileptic seizures, Magn. Reson. Imaging 18 (2000) 875–879, http://dx.doi.org/10.1016/S0730-725X(00)00183-1.
[122] H.G. Fujii, H. Sato-Akaba, M.C. Emoto, K. Itoh, Y. Ishihara, H. Hirata, Non-invasive mapping of the redox status in septic mouse by in vivo electron paramagnetic resonance imaging, Magn. Reson. Imaging 31 (2013) 130–138, http://dx.doi.org/10.1016/j.mri.2012.06.021.
[123] H. Yokayama, O. Itoh, H. Ohya-Nishiguchi, H. Kamada, Reducing ability of the striatum and cerebral cortex in rats following acute administration of risperidone or haloperidol: an estimation by *in vivo* electron paramagnetic resonance imaging, Neurochem. Res. 27 (2002) 243–248, http://dx.doi.org/10.1023/A:1014840722626.
[124] H. Yokoyama, S.-I. Ishida, T. Ogata, In vivo temporal EPR study using a region-selected intensity determination method to estimate cerebral reducing ability in rats treated with olanzapine, Magn. Reson. Imaging 28 (2010) 898–902, http://dx.doi.org/10.1016/j.mri.2010.03.019.
[125] P. Kuppusamy, J.L. Zweier, Cardiac applications of EPR imaging, NMR Biomed. 17 (2004) 226–239, http://dx.doi.org/10.1002/nbm.912.
[126] S.S. Leonard, K. Mowrey, D. Pack, X. Shi, V. Castranova, P. Kuppusamy, V. Vallyathan, *In vivo* bioassays of acute asbestosis and its correlation with ESR spectroscopy and imaging in redox status, Mol. Cell. Biochem. 234/235 (2002) 369–377, http://dx.doi.org/10.1023/A:1015919101174.
[127] J.-Y. Han, K. Takeshita, H. Utsumi, Noninvasive detection of hydroxyl radical generation in lung by diesel exhaust particles, Free Radic. Biol. Med. 30 (2001) 516–525, http://dx.doi.org/10.1016/S0891-5849(00)00501-3.
[128] M.K. Ahsan, H. Nakamura, M. Tanito, K. Yamada, H. Utsumi, J. Yodoi, Thioredoxin-1 suppresses lung injury and apoptosis induced by diesel exhaust particles (DEP) by scavenging reactive oxygen species and by inhibiting DEP-induced downregulation of Akt, Free Radic. Biol. Med. 39 (2005) 1549–1559, http://dx.doi.org/10.1016/j.freeradbiomed.2005.07.016.
[129] K. Takeshita, A. Hamada, H. Utsumi, Mechanisms related to reduction of radical in mouse lung using an L-band ESR spectrometer, Free Radic. Biol. Med. 26 (1999) 951–960, http://dx.doi.org/10.1016/S0891-5849(98)00278-0.
[130] S. Matsumoto, I. Koshiishi, T. Inoguchi, H. Nawata, H. Utsumi, Confirmation of superoxide generation via xanthine oxidase in streptozotocin-induced diabetic mice, Free Radic. Res. 37 (2003) 767–772, http://dx.doi.org/10.1080/1071576031000107344.
[131] T. Sonta, T. Inoguchi, H. Tsubouchi, N. Sekiguchi, K. Kobayashi, S. Matsumoto, H. Utsumi, H. Nawata, Evidence for contribution of vascular NAD(P)H oxidase to increased oxidative stress in animal models of diabetes and obesity, Free Radic. Biol. Med. 37 (2004) 115–123, http://dx.doi.org/10.1016/j.freeradbiomed.2004.04.001.
[132] T. Sonta, T. Inoguchi, S. Matsumoto, K. Yasukawa, M. Inuo, H. Tsubouchi, N. Sonoda, K. Kobayashi, H. Utsumi, H. Nawata, In vivo imaging of oxidative stress in the kidney of diabetic mice and its normalization by angiotensin II type 1 receptor blocker, Biochem. Biophys. Res. Commun. 330 (2005) 415–422, http://dx.doi.org/10.1016/j.bbrc.2005.02.174.
[133] H. Tsubouchi, T. Inoguchi, T. Sonta, N. Sato, N. Sekiguchi, K. Kobayashi, H. Sumimoto, H. Utsumi, H. Nawata, Statin attenuates high glucose-induced and diabetes-induced oxidative stress in vitro and in vivo evaluated by electron spin resonance measurement, Free. Radic. Biol. Med. 39 (2005) 444–452, http://dx.doi.org/10.1016/j.freeradbiomed.2005.03.031.
[134] H.P. Kobayashi, T. Watanabe, S. Oowada, A. Hirayama, S. Nagase, M. Kamibayashi, T. Otsubo, Effect of CV159–Ca^{2+}/calmodulin blockade on redox status hepatic ischemia–reperfusion injury in mice evaluated by a newly developed *in vivo* EPR imaging technique, J. Surg. Res. 147 (2008) 41–49, http://dx.doi.org/10.1016/j.jss.2007.06.024.
[135] A. Hirayama, S. Nagase, A. Ueda, T. Oteki, K. Takada, M. Obara, M. Inoue, K. Yoh, K. Hirayama, A. Koyama, In vivo imaging of oxidative stress in ischemia-reperfusion renal injury using electron paramagnetic resonance, Am. J. Physiol. – Ren. Physiol. 288 (2005) F597–F603, http://dx.doi.org/10.1152/ajprenal.00020.2004.
[136] N. Phumala, T. Ide, H. Utsumi, Noninvasive evaluation of in vivo free radical reactions catalyzed by iron content using in vivo ESR spectroscopy, Free Radic. Biol. Med. 26 (1999) 1209–1217, http://dx.doi.org/10.1016/S0891-5849(98)00314-1.
[137] A. Hirayama, A. Ueda, T. Oteki, S. Nagase, K. Aoyagi, A. Koyama, *In vivo* imaging of renal redox status during azelnidipine treatment, Hypertens. Res. 31 (2008) 1643–1650, http://dx.doi.org/10.1291/hypres.31.1643.
[138] A. Hirayama, K. Yoh, S. Nagase, A. Ueda, K. Itoh, N. Morito, K. Hirayama, S. Takahashi, M. Yamamoto, A. Koyama, EPR imaging of reducing activity in Nrf2 transcriptional factor-deficient mice, Free Radic. Biol. Med. 34 (2003) 1236–1242, http://dx.doi.org/10.1016/S0891-5849(03)00073-X.
[139] H. Togashi, K. Oikawa, T. Adachi, K. Sugahara, J. Ito, T. Takeda, H. Watanabe, K. Saito, T. Saito, T. Fukui, H. Takeda, H. Ohya, S. Kawata, Mucosal sulfhydryl compounds evaluation by in vivo electron spin resonance spectroscopy in mice with experimental colitis, Gut 52 (2003) 1291–1296, http://dx.doi.org/10.1136/gut.52.9.1291.
[140] Y. Miura, K. Anzai, S. Urano, T. Ozawa, *In vivo* electron paramagnetic resonance studies on oxidative stress caused by X-irradiation in whole mice, Free Radic. Biol. Med. 23 (1997) 533–540, http://dx.doi.org/10.1016/S0891-5849(97)00103-2.
[141] P. Kuppusamy, M. Afeworki, R.A. Shankar, D. Coffin, M.C. Krishna, S.M. Hahn, J.B. Mitchell, J.L. Zweier, *In vivo* electron paramagnetic resonance imaging of tumor heterogeneity and oxygenation in a murine model, Cancer Res. 58 (1998) 1562–1568.
[142] P. Kuppusamy, H. Li, G. Ilangovan, A.J. Cardounel, J.L. Zweier, K. Yamada, M. C. Krishna, J.B. Mitchell, Noninvasive imaging of tumor redox status and its modification by tissue glutathione level, Cancer Res. 62 (2002) 307–312.
[143] G. Ilangovan, H. Li, J.L. Zweier, M.C. Krishna, J.B. Mitchell, P. Kuppusamy, In vivo measurement of regional oxygenation and imaging of redox status in RIF-1 murine tumor: effect of carbogen-breathing, Magn. Reson. Med. 48 (2002) 723–730, http://dx.doi.org/10.1002/mrm.10254.
[144] K. Takeshita, K. Kawaguchi, K. Fujii-Akawa, M. Ueno, S. Okazaki, M. Ono, M. C. Krishna, P. Kupussamy, T. Ozawa, N. Ikota, Heterogeneity of regional redox status and relation of the redox status to oxygenation in a tumor model, evaluated using electron paramagnetic resonance imaging, Cancer Res. 70 (2010) 4133–4140, http://dx.doi.org/10.1158/0008-5472.CAN-09-4369.
[145] Z. Zhelev, V. Gadjeva, I. Aoki, R. Bakalova, T. Saga, Cell-penetrating nitroxides as molecular sensors for imaging of cancer in vivo, based on tissue redox activity, Mol. Biosyst. 8 (2012) 2733–2740, http://dx.doi.org/10.1039/c2mb25128k.
[146] R. Bakalova, Z. Zhelev, I. Aoki, T. Saga, Tissue redox activity as a hallmark of carcinogenesis: from early to terminal stages of cancer, Clin. Cancer Res. 19 (2013) 2503–2517, http://dx.doi.org/10.1158/1078-0432.CCR-12-3726.
[147] F. Hyodo, S. Ito, K. Yasukawa, R. Kobayashi, H. Utsumi, Simultaneous and spectroscopic redox molecular imaging of multiple free radical intermediates using dynamic nuclear polarization-magnetic resonance imaging, Anal. Chem. 86 (2014) 7234–7238, http://dx.doi.org/10.1021/ac502150x.
[148] Y. Kinoshita, K.-I. Yamada, T. Yamasaki, H. Sadasue, K. Sakai, H. Utsumi, Development of novel nitroxyl radicals for controlling reactivity with ascorbic acid, Free Radic. Res. 43 (2009) 565–571, http://dx.doi.org/10.1080/10715760902914575.
[149] A.A. Bobko, O.V. Efimova, M.A. Voinov, V.V. Khramtsov, Unique oxidation of imidazolidine nitroxides by potassium ferricyanide: strategy for designing paramagnetic probes with enhanced sensitivity to oxidative stress, Free Radic. Res. 46 (2012) 1115–1122, http://dx.doi.org/10.3109/10715762.2012.692785.
[150] J.T. Paletta, M. Pink, B. Foley, S. Rajca, A. Rajca, Synthesis and reduction kinetics of sterically shielded pyrrolidine nitroxides, Org. Lett. 14 (2012) 5322–5325, http://dx.doi.org/10.1021/ol302506f.
[151] A.P. Jagtap, I. Krstic, N.C. Kunjir, R. Hänsel, T.F. Prisner, S.T. Sigurdsson, Sterically shielded spin labels for in-cell EPR spectroscopy: analysis of stability in reducing environment, Free Radic. Res. 49 (2015) 78–85, http://dx.doi.org/10.3109/10715762.2014.979409.
[152] Y. Liu, Y. Song, F. De Pascali, X. Liu, F.A. Villamena, J.L. Zweier, Tetrathiatriarylmethyl radical with a single aromatic hydrogen as a highly sensitive and specific superoxide probe, Free Radic. Biol. Med. 53 (2012) 2081–2091, http://dx.doi.org/10.1016/j.freeradbiomed.2012.09.011.
[153] G. Redler, E.D. Barth, K.S. Bauer Jr., J.P.Y. Kao, G.M. Rosen, H.J. Halpern, In vivo electron paramagnetic resonance imaging of differential tumor targeting using *cis*-3,4-di(acetoxymethoxycarbonyl)-2,2,5,5-tetramethyl-1-pyrrolidinyloxyl, Magn. Reson. Med. 71 (2014) 1650–1656, http://dx.doi.org/10.1002/mrm.24813.